

Reviews

Trends in Cyclopentadienyl–Main-Group-Metal Bonding[†]

Peter H. M. Budzelaar*

Department of Inorganic Chemistry, University of Nijmegen, Toernooiveld 1,
6525 ED Nijmegen, The Netherlands

Jeroen J. Engelberts and Joop H. van Lenthe[‡]

Theoretical Chemistry Group, Debye Institute, Utrecht University, Padualaan 14,
3584 CH Utrecht, The Netherlands

Received November 7, 2002

In contrast to transition metals (TMs), main-group metals (MMs) show a bewildering variety of bonding arrangements to cyclopentadienyl (Cp) groups, including electron-precise, electron-excess, and electron-deficient structures. From a theoretical examination of a large number of representative species, and a comparison with experimental structures, we have deduced three factors which combine to produce this variety. (1) The drive toward electron-precise structures is caused by the preference for electronic saturation (8e rule, similar to the TM 18e rule). (2) A high degree of ionicity leads (if space permits) to increased hapticity and hence to excess-electron structures; this is seen in complexes of Li, Na, Mg, and Al and, to a lesser extent, Pb and Bi. (3) The metal *ns* orbital has a preference for forming σ -bound structures. Thus, heavy involvement of this orbital in the bonding leads to a preference for σ -bound structures, even if these are electron-deficient. This last factor, in particular, leads to the paradoxical situation that adding a donor can increase the hapticity of the system. An examination of the slippage curves for a large number of systems shows that Cp–MM interactions are generally much “softer” than the corresponding Cp–TM interactions, leading to easy accessibility of a wide range of geometrical arrangements for many compounds. For intermediate-hapticity structures, valence-bond calculations indicate that the general preference for η^2 over η^3 structures is primarily due to ionic and σ bond interactions, the latter having a better orbital size match in the η^2 situation.

Introduction

Cyclopentadienyl ligands are traditionally associated with transition metals. Typically, transition metals form a strong, covalent, and symmetric η^5 bond to a cyclopentadienyl (Cp) group. In contrast, main-group metals show a bewildering variety of bonding arrangements, from symmetric η^5 via various slipped η^x structures all the way to pure σ -bound, as well as numerous bridging modes; there is no single clearly preferred structural type.^{1a}

In the transition-metal series, the few exceptions to the η^5 -bound situation that exist are easily explained on the basis of electron-counting rules. For main-group metals, no such uniform rules seem to exist. This is

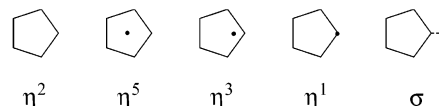


Figure 1. Idealized representations of Cp–metal bonding arrangements. In the order shown, they illustrate the slippage of the metal over the Cp ring.

illustrated by the series of Cp_2M^+ complexes of the group 13 metals,² where (according to calculations and, in part, confirmed by experiments) on going down the periodic table the structure changes from $\eta^5:\eta^1$ (B; electron precise) to $\eta^5:\eta^5$ (Al; electron excess) back to $\eta^5:\eta^1$ (Ga, In; electron precise) and then to $\eta^1:\eta^1$ (Tl; electron deficient). Kwon and McKee recently reviewed theoretical studies of main-group-metal sandwich and half-sandwich complexes.^{1b} Rayón and Frenking have analyzed the bonding between main-group metals and cyclopentadienyl groups in terms of electrostatic and orbital contributions.^{1c} They concluded that, except for boron, electrostatic interactions dominate the inter-

* To whom correspondence should be addressed. E-mail: budz@sci.kun.nl.

[†] Dedicated to Prof. Dr. G. J. M. van der Kerk on the occasion of his 90th birthday.

[‡] E-mail: joop@chem.uu.nl.

(1) (a) For a recent review, see Jützi, P.; Burford, N. *Chem. Rev.* **1999**, *99*, 969. (b) Kwon, C.; McKee, M. L. Main-Group Half-Sandwich and Full-Sandwich Metallocenes. In *Computational Organometallic Chemistry*; Cundari, T. R., Ed.; Marcel Dekker: New York, 2001; p 397ff. (c) Rayón, V. M.; Frenking, G. *Chem. Eur. J.* **2002**, *8*, 4693.

(2) Macdonald, C. L. B.; Gorden, J. D.; Voigt, A.; Cowley, A. H. *J. Am. Chem. Soc.* **2000**, *122*, 11725.

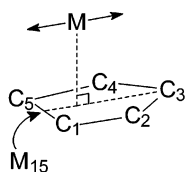


Figure 2. Definition of “reaction coordinate” for ring slippage curves. M_{15} is the midpoint of the C_1 – C_5 bond; the projection of the metal M on the $C_1C_3C_5$ plane is dragged along the C_3 – M_{15} vector.

action energy and are more important (at least in a relative sense) than in the transition series.

For many specific cases, observed structures have been rationalized on the basis of qualitative or quantitative MO arguments. While such explanations are certainly useful, they do not help much in understanding the trends in Cp–M bonding arrangements observed throughout the periodic table. In the current paper, we try to rectify this situation by studying a large series of Cp–main-group-metal complexes theoretically. We have not only focused on the most stable arrangement in each case but also have explicitly calculated the ring-slippage potential-energy curves. The advantage of such an approach is that it allows one to estimate the extent to which packing effects and substituents can influence the observed structures. This makes the conclusions more generally applicable.

In the present contribution, we concentrate on *monomeric* cyclopentadienyl derivatives. The formation of polymeric structures in the solid state, which is so typical for main-group metals, is only touched upon briefly, since it will be discussed in more detail in a separate paper.

Methods

Geometries and Slippage Curves. All structures were optimized at the B3LYP level³ using the GAMESS-UK package.⁴ Most structures were optimized within C_s symmetry to allow separate calculation of η^2 - and η^3/η^1 -like structures. For definition of the “reaction coordinate” used for slippage curve calculations, see Figure 2: the projection of the metal atom on the $C_1C_3C_5$ plane was dragged along the M_{15} – C_3 line in intervals of 0.3 Å, and the system was again restricted to C_s symmetry (mirror plane through M , C_3 , and M_{15}). No other constraints were used.

All calculations involving first- and second-row main-group metals (Li–Si) used the 6-31G* basis set.⁵ For calculations involving heavier atoms, we used the small split-valence 3-21G basis⁶ on C and H and a split-valence basis with small-core pseudopotential (LANL2DZ⁷) on the metal.

(3) (a) Lee, C.; Yang, W.; Parr, R. G. *Phys. Rev. B* **1988**, *37*, 785. (b) Becke, A. D. *J. Chem. Phys.* **1993**, *98*, 1372. (c) Becke, A. D. *J. Chem. Phys.* **1993**, *98*, 5648.

(4) GAMESS-UK is a package of ab initio programs, written by: Guest, M. F.; Van Lenthe, J. H.; Kendrick, J.; Schoffel, K.; Sherwood, P. with contributions from Amos, R. D.; Buenker, R. J.; Van Dam, H. J. J.; Dupuis, M.; Handy, N. C.; Hillier, I. H.; Knowles, P. J.; Bonacic-Koutecky, V.; Von Niessen, W.; Harrison, R. J.; Rendell, A. P.; Saunders, V. R.; Stone, A. J.; De Vries, A. H. The package is derived from the original GAMESS code of: Dupuis, M.; Spangler, D.; Wendoloski, J. NRCC Software Catalog, Vol. 1, Program No. QG01 (GAMESS), 1980. DFT module by P. Young, under the auspices of the EPSRC's Collaborative Computational Project No. 1 (CCP1) (1995–1997).

(5) Hariharan, P. C.; Pople, J. A. *Theor. Chem. Acta* **1973**, *28*, 213. Francl, M. C.; Pietro, W. J.; Hehre, W. J.; Binkley, J. S.; Gordon, M. S.; Defrees, D. J.; Pople, J. A. *J. Chem. Phys.* **1982**, *77*, 3654.

Table 1 lists the calculated preferred structures of all species studied, together with relevant alternatives; Table 2 summarizes data obtained from the slippage curves (total energies for optimized structures and slippage curves are available as Supporting Information, Tables S1 and S2). The inner (r_φ) and outer (R_φ) limits for movement of the metal atom away from its central position above the ring, accessible within a pre-defined energy range, were obtained by interpolation from the slippage curves. $\varphi = 0$ corresponds to movement toward C_3 , i.e., $\eta^3/\eta^1/\sigma$ slippage, and $\varphi = \pi/5$ to movement toward M_{15} , i.e., η^2 slippage. For intermediate values of φ we assumed a linear dependence of r_φ and R_φ on φ . Integration leads to different expressions for the accessible area, depending on the shape of the accessible region (see Figure 3 for shape definitions):⁸

$$\text{central area: } \pi \left[R_0 R_{\pi/5} + \frac{1}{3} (R_0 - R_{\pi/5})^2 \right]$$

peripheral area:

$$\pi \left[R_0 R_{\pi/5} + \frac{1}{3} (R_0 - R_{\pi/5})^2 - r_0 r_{\pi/5} - \frac{1}{3} (r_0 - r_{\pi/5})^2 \right]$$

local area:

$$\frac{\pi (R_0^2 - r_0^2)^2}{2R_0^2}$$

Valence-Bond Calculations. The molecules CpAlH₂, CpSiH, and CpSiH₃ were also studied using valence-bond calculations with the Turtle program⁹ as incorporated in the GAMESS-UK package.⁴ In these studies, the 6-31G basis was used for the carbon and hydrogen atoms, while for the metal atoms the 6-31G* basis was used. The geometries of the DFT calculations were used without further geometry optimization.

We wanted to analyze the bonding between the metal hydride moiety (MH_x) and the Cp group. Thus, we considered the molecule as split into the corresponding two fragments. We created different bonding arrangements of the two fragments by means of (electronic) VB structures. For CpSiH and CpAlH₂ we chose three different structures (shown schematically in Figure 11): (i) an ionic structure, combining of Cp[−] and MH_x⁺, (ii) a σ -bonded structure, with a singly occupied sp_x orbital on MH_x and a singly occupied π -orbital on the Cp ring, and (iii) a π -bonded structure, with a singly occupied p_z orbital on MH_x and a singly occupied π -orbital on the Cp ring.

We did not include a π -bonded structure for CpSiH₃, because Si does not have a low-lying empty p_z orbital in the SiH₃ fragment. The alternative ionic structure consisting of Cp⁺ and MH_x[−] was found to be too high in energy to contribute significantly.

A RHF calculation on each fragment yielded the inner shell orbitals: i.e., the C 1s and the metal 1s, 2s, and 2p orbitals. We obtained the C–C, C–H, and M–H σ -orbitals from a localization¹⁰ of the remaining RHF orbitals. All these orbitals were doubly occupied in all structures; the C–H and M–H orbitals were frozen. Starting combinations for the orbitals relevant to the bonding (the C–C π -orbitals, the metal sp_x and p_z orbitals, and the Si lone pair) were made by hand. These orbitals were optimized in the total wave function with VBSCF^{11,12} and were allowed to be different for each structure.

(6) Binkley, J. S.; Pople, J. A.; Hehre, W. J. *J. Am. Chem. Soc.* **1980**, *102*, 939.

(7) (a) Hay, P. J.; Wadt, W. R. *J. Chem. Phys.* **1985**, *82*, 270. (b) Wadt, W. R.; Hay, P. J. *J. Chem. Phys.* **1985**, *82*, 284. (c) Hay, P. J.; Wadt, W. R. *J. Chem. Phys.* **1985**, *82*, 299.

(8) For the local-area case, $R_{\pi/5}$ and $r_{\pi/5}$ do not exist and we need another assumption about the behavior of R_φ as a function of φ . We assumed $\varphi(r_\varphi = R_\varphi) = (1 - r_0/R_0)\pi/5$ and again linear dependence of R_φ on φ .

(9) Verbeek, J.; Langenberg, J. H.; Byrman, C. P.; Dijkstra, F.; Engelberts, J. J.; van Lenthe, J. H. Turtle, an ab Initio VB/VBSCF Program; Utrecht, the Netherlands, 1988–2002.

(10) Foster, J. M.; Boys, S. F. *Rev. Mod. Phys.* **1960**, *32*, 300–302.

Table 1. Calculated Structures of Main-Group-Metal Cyclopentadienyls

group	element	species	structure	E_{rel}^a	M-Cp ^b	M-Cg ^b	slip ^b	exptl ^c	
1	Li	CpLi	$C_{5v} \eta^5$		1.73 (1.92; 1.79, 1.80)	1.73 (1.92; 1.79, 1.80)	0 (0.05; 0.01, 0.04)	(MeC ₅ H ₄)Li(TMEDA); ^{17d} (Me ₃ Si) ₃ C ₅ H ₂ Li(THF) ^{17f}	
		Cp ₂ Li ⁻	$D_{5d} \eta^5: \eta^5$		2.01 (2.01); 1.97, 1.99)	2.01 (2.01); 1.97, 1.99)	0 (0.10; 0.07, 0.10)	Ph ₄ P ⁺ Cp ₂ Li ⁻ ; ^{19a} TAS ⁺ Cp ₂ Li ⁻ ¹⁸	
	Na	CpNa	$C_{5v} \eta^5$		2.19 (2.40; 2.50)	2.19 (2.40; 2.51)	0 (0.06; 0.17)	(Me ₅ C ₅)Na(Py) ₃ ; ^{17j} (Me ₃ Si) ₃ C ₅ H ₂ Na(pmdta) ^{17k}	
		Cp ₂ Na ⁻	$D_{5d} \eta^5: \eta^5$		2.37 (2.36; 2.33)	2.37 (2.37; 2.33)	0 (0.10; 0.05)	Ph ₄ P ⁺ Cp ₂ Na ⁻ ; ^{19b} [(TAS) ₂ Cp] ⁺ Cp ₂ Na ⁻ ¹⁸	
2	Be	CpBe ⁺	$C_{5v} \eta^5$		1.37	1.37	0		
		CpBeH	$C_{5v} \eta^5$		1.53	1.53 (1.50)	0	CpBeMe ²¹	
		Cp ₂ Be	$C_s \eta^5: \eta^1$	(0)	1.53 (1.51), 1.75 (1.84)	1.53 (1.51), 2.36 (2.26)	0.03 (0.05), 1.59 (1.31)	Cp ₂ Be ^{23c}	
			$C_{2h} \eta^3: \eta^3$ ^d	1.8	1.68	1.69	0.19		
	Mg	CpMg ⁺	$C_{5v} \eta^5$		1.88	1.88	0		
		CpMgH	$C_{5v} \eta^5$		2.02	2.02 (2.00)	0	CpMg/BU ²²	
		Cp ₂ Mg	$D_{5d} \eta^5: \eta^5$		2.03 (1.99)	2.03 (1.99)	0 (0.03)	Cp ₂ Mg ²⁰	
		CpCu	$C_{5v} \eta^5$		1.90	1.90	0		
11	Cu	CpCu-PH ₃	$C_s (\sim C_{5v}) \eta^5$		1.91 (1.86; 1.90)	1.91 (1.86; 1.90)	0.00 (0.04; 0)	CpCuPPh ₃ ; ^{26a} CpCuPET ₃ ^{26b}	
		CpAg	$C_s \eta^1$	(0)	2.18	2.70	1.60		
			$C_s \eta^2$	0.8	2.20	2.58	1.36		
		CpAg-PH ₃	$C_s (\sim C_{5v}) \eta^5$		2.20 (2.22, 2.24)	2.20 (2.35, 2.26)	0.13 (0.77, 0.30)	((Me ₃ Si) ₃ C ₅ H ₂)Ag-(P <i>n</i> Bu ₃) ²⁷	
	Au	CpAu	$C_s \eta^1$	(0)	1.93	2.85	2.10		
			$C_s \eta^2$	8.1	2.10	2.64	1.61		
		CpAu-PH ₃	$C_s \eta^1$	(0)	2.10 (2.15)	2.73 (2.61)	1.75 (1.48)	CpAuP <i>i</i> Pr ₃ ^{28a}	
			$C_s \eta^2$	3.9	2.19	2.49	1.19		
12	Zn	CpZn ⁺	$C_s \eta^2$	(0)	1.99	2.50	1.52		
			$C_s \eta^1$	3.3	2.03	2.64	1.68		
			$\sim C_{5v} \eta^5$	8.0	1.88	1.88	0.01		
		CpZnH	$C_{5v} \eta^5$		2.03 (-; 2.01, 2.02; -; 2.06, 2.03)	2.03 (1.93; 2.02, 2.02; 2.00; 2.08, 2.05)	0 (-; 0.26, 0.10; -; 0.28, 0.25)	CpZnMe; ^{29a} CpCo(PPh ₃)(ZnZn) ₂ ; ^{29b} Cp ₂ NbH ₂ ZnZn; ^{29c} Cp' ₂ TaH(ZnZn) ₂ ^{29d}	
		Cd	CpZnH ₂ ⁻	$C_s \eta^2$	(0)	2.28	2.58	1.20	
				$C_s \eta^1$	0.9	2.32	2.56	1.08	
			Cp ₂ Zn	$C_{2h} \eta^3: \eta^3$	(0)	2.06 (1.84, 2.11; 1.83, 2.21; 1.93; 1.91)	2.13 (1.85, 2.42; 1.90, 2.67; -; -)	0.53 (0.20, 1.18; 0.52, 1.51; -; -)	(PhMe ₄ C ₅) ₂ Zn; ^{31c} (<i>i</i> Pr ₄ C ₅ H) ₂ Zn; ^{31d} (Me ₃ SiC ₅ H ₄) ₂ Zn; ^{31b} (Me ₅ C ₅) ₂ Zn ^{31b,e}
				$D_{5d} \eta^5: \eta^5$	0.7	2.04	2.04	0	
		Hg	CpCd ⁺	$C_s \eta^2$	(0)	2.22	2.72	1.58	
				$C_s \eta^1$	2.3	2.24	2.83	1.73	
			CpCdH	$C_{5v} \eta^5$		2.24	2.24	0	
			Cp ₂ Cd	$C_{2h} \eta^3: \eta^3$	(0)	2.27	2.37	0.68	
	Hg		$D_{5d} \eta^5: \eta^5$	0.9	2.24	2.24	0		
		CpHg ⁺	$C_s \eta^2$	(0)	2.34	2.90	1.72		
			$C_s \eta^1$	0.3					
		CpHgH	$C_s \eta^1$	(0)	2.36	2.59	1.06		
	B		$C_s \eta^2$	0.9	2.36	2.51	0.85		
		Cp ₂ Hg	$C_{2h} \sigma: \sigma$	(0)	2.32 (1.99, 2.01)	2.76 (2.84, 2.86)	1.50 (2.03, 2.03)	Cp ₂ Hg ^{33a}	
			$D_{5d} \eta^5: \eta^5$	22.6	2.32	2.32	0		
		CpBH ⁺	$C_{5v} \eta^5$		1.25 (1.15, 1.22)	1.25 (1.15, 1.22)	0 (0.01, 0.07)	Me ₅ C ₅ BBr ⁺ AlBr ₄ ⁻ ^{40c}	
	Al	CpBH ₂	$C_s \eta^2$	(0)	1.56	2.01	1.27		
			$C_s \eta^1$	2.0	1.59	2.24	1.58		
		CpBCl ₂	$C_s \eta^1$	(0)	1.37 (1.60)	2.50 (2.22)	2.09 (1.54)	Me ₅ C ₅ BClAsfBu ₂ ⁴¹	
			$C_s \eta^2$	5.9	1.52	2.09	1.43		
	B	CpBMe ₂	$C_s \eta^1$	(0)	1.50	2.45	1.94		
			$C_s \eta^2$	3.7	1.57	2.12	1.43		
		Cp ₂ B ⁺	$C_s \eta^5: \eta^1$	(0)	1.28 (1.29), 1.33 (1.49)	1.28 (1.29), 2.50 (2.40)	0.01 (0.02), 2.12 (1.87)	(Me ₅ C ₅) ₂ B ⁺ AlBr ₄ ⁻ ^{40e}	
			$D_{5d} \eta^5: \eta^5$	53.9	1.52	1.52	0		
13	Al	CpAl	$C_{5v} \eta^5$		2.06 (2.06; 2.01)	2.06 (2.06; 2.01)	0 (0; 0.05)	Me ₅ C ₅ Al; ^{34b} (Me ₅ C ₅ Al) ₄ ^{34c,f}	
		CpAlH ⁺	$C_{5v} \eta^5$		1.77	1.77	0.00		
		CpAlH ₂	$C_s \eta^2$	(0)	2.01	2.26	1.04		
			$C_s \eta^3$	1.6	2.01	2.08	0.56		
		CpAlMe ₂	$C_s \eta^2$	(0)	2.03 (~2.13)	2.34	1.17 (~0.96)	CpAlMe ₂ ^{42a}	
			$C_s \eta^3$	2.4	2.05	2.15	0.65		
		CpAlCl ₂	$C_s \eta^3 \rightarrow \eta^5$	(0)	1.90 (1.92)	1.90 (1.92)	0.01 (0.13)	CpAl(OAr) ₂ ^{42d}	
			$C_s \eta^2$	0.8	1.96	2.27	1.16		
		CpAlH ₃ ⁻	$C_s \eta^1$	(0)	2.01	2.86	2.03		
			$C_s \eta^2$	5.1	2.20	2.66	1.50		
		CpAlCl ₃ ⁻	$C_s \eta^1$	(0)	1.88 (2.02)	2.82 (2.58)	2.10 (1.61)	Me ₅ C ₅ AlCl ₃ ⁻ (Me ₅ C ₅) ₂ Al ⁺ ^{42h}	
			$C_s \eta^2$	7.4	2.10	2.54	1.43		
	Ga	Cp ₂ Al ⁺	$D_{5d} \eta^5: \eta^5$		1.82 (1.78)	1.82 (1.78)	0 (0.03)	(Me ₅ C ₅) ₂ Al ⁺ Me ₅ C ₅ AlCl ₃ ⁻ ^{42h}	
		Cp ₂ AlH	$C_2 (\sim C_{2v}) \eta^2$		2.05 (2.04, 2.03)	2.27 (2.33, 2.21)	0.99 (1.13, 0.87)	Cp ₂ AlMe ^{42p}	
		CpGa	$C_{5v} \eta^5$		2.18 (2.08; 2.08)	2.18 (2.08; 2.08)	0 (0; 0.04)	Me ₅ C ₅ Ga; ^{35c} (Me ₅ C ₅ Ga) ₆ ^{35b}	

Table 1. (Continued)

group	element	species	structure	E_{rel}^a	M–Cp ^b	M–Cg ^b	slip ^b	exptl ^c
13	Ga	CpGaH ⁺	$C_{5v} \eta^5$		1.85	1.85	0	
		CpGaH ₂	$C_s \eta^2$	(0)	2.05	2.38	1.20	
			$C_s \eta^3$	2.4	2.09	2.40	1.18	
		Cp ₂ Ga ⁺	$C_s \eta^5: \eta^1$	(0)	1.89 (1.97), 1.93 (1.65)	1.89 (2.13), 2.60 (2.85)	0.11 (0.81), 1.74 (2.33)	[(Me ₅ C ₅) ₂ Ga ⁺ BF ₄ ⁻] ₂ ²
	In	Cp ₂ GaH	$D_{5d} \eta^5: \eta^5$	7.5	1.91	1.91	0	
		CpIn	$C_2 \eta^{1.5}$		2.09	2.38	1.14	
			$C_{5v} \eta^5$		2.36 (2.32; 2.31; 2.29; 2.30)	2.36 (2.32; 2.31; 2.29; 2.30)	0 (0; 0; 0; 0.04)	CpIn; ^{36d} Me ₅ C ₅ H ₄ In; ^{36d} Me ₅ C ₅ In; ^{36e} (Me ₅ C ₅ In) ₆ ^{36b,e}
		CpInH ⁺	$C_{5v} \eta^5$		2.06	2.06	0	
		CpInH ₂	$C_s \eta^2$	(0)	2.25	2.53	1.16	
			$C_s \eta^3$	1.7	2.28	2.49	1.01	
		Cp ₂ In ⁺	$C_s \eta^5: \eta^1$	(0)	2.09	2.09	0.12	
			$D_{5d} \eta^5: \eta^5$	6.6	2.09	2.09	0	
		Cp ₂ InH	$C_2 (\sim C_{2v}) \eta^2$		2.27	2.50	1.05	
		CpTl	$C_{5v} \eta^5$		2.52 (2.41; 2.37; 2.49; 2.49)	2.52 (2.41; 2.37; 2.49; 2.49)	0 (0; 0; 0.03; 0.13)	CpTl; ^{37a} Me ₅ C ₅ Tl; ³⁷ⁱ Bz ₅ C ₅ Tl; ^{37h} (Bz ₅ C ₅ Tl) ₂ ^{37h}
14	Si	CpTlH ⁺	$C_s \eta^1$	(0)	2.31	2.55	1.10	
			$C_s \eta^2$	1.1	2.31	2.50	0.97	
		CpTlH ₂	$C_s \eta^2$	(0)	2.41	2.68	1.17	
			$C_s \eta^3$	1.0	2.43	2.68	1.13	
		Cp ₂ Tl ⁺	$C_s \eta^1: \eta^1$		2.36	2.76	1.45	
			$D_{5d} \eta^5: \eta^5$	43.5	2.23	2.23	0	
		Cp ₂ TlH	$C_2 \eta^{1.5}: \eta^{1.5}$		2.43	2.69	1.14	
		CpSi ⁺	$C_{5v} \eta^5$		1.82	1.82	0	
		CpSiH	$C_s \eta^2$	(0)	2.00	2.29	1.12	
			$C_s \eta^1$	1.8	2.00	2.17	0.82	
	CpSiH ₃	$C_s \eta^1$	(0)	1.74 (1.52)	2.74 (2.86)	2.12 (2.42)	ArMe ₂ C ₅ H ₂ SiMe ₃ ^{53h}	
		$C_s \eta^2$	14.3	1.97	2.42	1.41		
	Cp ₂ Si	$C_2 \eta^2: \eta^2$	(0)	2.13 (2.10, 2.11, 2.11)	2.24 (2.12, 2.12, 2.11)	0.69 (0.25, 0.22, 0.03)	(Me ₅ C ₅) ₂ Si ⁴⁹	
	Ge	CpGe ⁺	$D_{5d} \eta^5: \eta^5$	4.1	2.21	2.21	0	
CpGeH		$C_{5v} \eta^5$		2.01 (1.90)	2.01 (1.90)	0 (0.02)	Me ₅ C ₅ GeBF ₄ ^{47b}	
		$C_s \eta^2$	(0)	2.15 (2.11; 2.13; 2.02)	2.41 (2.24; 2.22; 2.07)	1.10 (0.74; 0.65; 0.43)	Me ₅ C ₅ GeCH(SiMe ₃) ₂ ^{48a} Me ₅ C ₅ GeC(SiMe ₃) ₃ ^{48b} Me ₅ C ₅ GeCl ^{48c}	
CpGeH ₃		$C_s \eta^1$	2.1	2.17	2.35	0.89		
Sn	CpGeH ₃	$C_s \eta^1$	(0)	1.86 (1.78)	2.80 (2.78)	2.10 (2.12)	CpGeH ₃ ^{53g}	
		$C_s \eta^2$	13.9	2.10	2.54	1.44		
	Cp ₂ Ge	$C_2 \eta^3: \eta^3?$	(0)	2.28 (2.19)	2.31 (2.23)	0.41 (0.44)	Cp ₂ Ge ⁵⁰	
		$D_{5d} \eta^5: \eta^5$	0.6	2.30	2.30	0		
	CpSn ⁺	$C_{5v} \eta^5$		2.19 (2.29; 2.16)	2.19 (2.29; 2.16)	0 (0.09; 0.05)	Cp ₃ Sn ₂ BF ₄ (THF); ⁴⁶ Me ₅ C ₅ SnBF ₄ ^{47c}	
	CpSnH	$C_s \eta^2$	(0)	2.32 (2.30; 2.24)	2.55 (2.34; 2.42)	1.06 (0.45; 0.90)	CpSnCl; ^{48g,g} Me ₅ C ₅ SnCl ^{48d}	
		$C_s \eta^1$	1.4	2.34	2.49	0.84		
	CpSnH ₃	$C_s \eta^1$	(0)	2.09	2.90	2.01	Ph ₃ CC ₅ H ₄ SnMe ₃ ⁵³ⁱ	
		$C_s \eta^2$	8.1	2.25	2.67	1.45		
	Cp ₂ Sn	$C_2 \eta^3: \eta^3?$	(0)	2.42 (2.40, 2.42)	2.45 (2.41, 2.44)	0.39 (0.21, 0.31)	Cp ₂ Sn ^{51a}	
Pb		$D_{5d} \eta^5: \eta^5$	1.9	2.46	2.46	0		
	CpPb ⁺	$C_{5v} \eta^5$		2.25 (2.26)	2.25 (2.27)	0 (0.09)	Me ₅ C ₅ PbBF ₄ ^{47d}	
	CpPbH	$C_s \eta^2$	(0)	2.41	2.59	0.95		
		$C_s \eta^1$	0.8	2.42	2.55	0.79		
	CpPbH ₃	$C_s \eta^1$	(0)	2.15	2.96	2.03	CpPbPh ₃ ^{53f}	
		$C_s \eta^2$	7.6	2.34	2.76	1.46		
	Cp ₂ Pb	$C_2 \eta^5: \eta^5?$	(0)	2.49 (2.50; 2.52)	2.50 (2.50; 2.52)	0.24 (0; 0.16)	Cp ₂ Pb; ^{52a} (Me ₅ C ₅) ₂ Pb ^{51a}	
		$D_{5d} \eta^5: \eta^5$	0.6	2.50	2.50	0		
	CpAsH ⁺	$C_s \eta^2$	(0)	1.98	2.36	1.29		
		$C_s \eta^1$	6.2	2.06	2.31	1.04		
15	As	CpAsH ₂	$C_s \eta^1$	(0)	1.87 (2.98)	2.86 (3.09)	2.17 (1.65)	Me ₅ C ₅ As <i>t</i> Bu ₂ ⁶⁰
			$C_s \eta^2$	17.0	2.20	2.61	1.40	
		Cp ₂ As ⁺	$C_2 \eta^2: \eta^2$	(0)	2.09 (2.07, 2.10)	2.37 (2.14, 2.17)	1.10 (0.54, 0.56)	(Me ₅ C ₅) ₂ As ⁺ BF ₄ ⁻ ⁵⁴
			$D_{5d} \eta^5: \eta^5$	6.5	2.19	2.19	0	
	Sb	Cp ₂ AsH	$C_1 \eta^1: \eta^1$		1.91	2.85	2.11	
		CpSbH ⁺	$C_s \eta^2$	(0)	2.18	2.52	1.28	
			$C_s \eta^1$	4.4	2.24	2.45	0.99	
		CpSbH ₂	$C_s \eta^1$	(0)	2.11 (2.09)	2.97 (2.99)	2.09 (2.14)	(Me ₅ C ₅ Sb) ₄ ⁶¹
			$C_s \eta^2$	10.4	2.33	2.73	1.42	
		Cp ₂ Sb ⁺	$C_2 \eta^2: \eta^2$	(0)	2.30 (2.27, 2.28; 2.31, 2.29)	2.42 (2.29, 2.30; 2.31, 2.29)	0.73 (0.33, 0.26; 0.11, 0.11)	(Me ₅ C ₅) ₂ Sb ⁺ AlI ₄ ⁻ ; ⁵⁵ (<i>t</i> Bu ₃ C ₅ H ₂) ₂ Sb ⁺ AlCl ₄ ⁻ ⁵⁵
	Bi	Cp ₂ SbH	$D_{5d} \eta^5: \eta^5$	1.2	2.34	2.34	0	
		Cp ₂ SbH	$C_1 \eta^1: \eta^1$		2.17 (2.12, 2.21)	2.93 (2.92, 2.81)	1.97 (2.01, 1.74)	Cp ₃ Sb ⁵⁷
		CpBiH ⁺	$C_s \eta^2$	(0)	2.26	2.54	1.16	
			$C_s \eta^1$	2.9	2.30	2.47	0.90	
CpBiH ₂		$C_s \eta^1$	(0)	2.23	2.97	1.97		
		$C_s \eta^2$	7.8	2.41	2.76	1.35		
Cp ₂ Bi ⁺		$D_{5d} \eta^5: \eta^5$		2.38 (2.40, 2.39)	2.38 (2.40, 2.39)	0 (0.07, 0.07)	(<i>t</i> Bu ₃ C ₅ H ₂) ₂ Bi ⁺ AlCl ₄ ⁻ ⁵⁶	
Cp ₂ BiH		$C_1 \eta^1: \eta^1$		2.33 (2.39, 2.36; 2.49, 2.51)	2.87 (2.74, 2.95; 2.52, 2.55)	1.68 (1.34, 1.78; 0.38, 0.36)	Cp ₃ Bi; ⁵⁸ (<i>t</i> Bu ₃ C ₅ H ₂) ₂ BiCl ⁶²	

Table 1. (Continued)

group	element	species	structure	E_{rel}^a	M–Cp ^b	M–Cg ^b	slip ^b	exptl ^c
7	Mn	CpMnH (HS)	$C_{5v} \eta^5$	2.08	2.08	2.08	0	
		Cp ₂ Mn (HS)	$D_{5d} \eta^5: \eta^5$	2.09 (2.05)	2.09 (2.05)	2.09 (2.05)	0 (0.12)	(Me ₃ SiC ₅ H ₄) ₂ Mn ⁶³
		CpMn(CO) ₃ (LS)	$C_s (\sim C_{5v}) \eta^5$	1.82 (1.77)	1.82 (1.77)	1.82 (1.77)	0.00 (0.01)	CpMn(CO) ₃ ⁶⁴
8	Fe	Cp ₂ Fe	$D_{5d} \eta^5: \eta^5$	1.73 (~1.63)	1.73 (~1.63)	1.73 (~1.63)	0 (~0.05)	Cp ₂ Fe ⁶⁵

^a Energy relative to most stable structure (kcal/mol). ^b Legend: M–Cp = perpendicular distance of M to least-squares Cp plane; Cg = center of gravity of Cp ring; slip = distance between Cg and perpendicular projection of M on Cp plane. Experimental data (where available) are given in parentheses. ^c Compound for which experimental data are available. ^d Transition state for η^1/η^5 ring “exchange”. ^e The four compounds for which experimental data are given all have the $\eta^5:\eta^1$ structure instead of the calculated $\eta^{2.5}:\eta^{2.5}$ structure. ^f Averaged over the four independent Cp*Al moieties. ^g This structure is probably disordered and unreliable.

To aid convergence, we determined these orbitals first for separate structures and combined them for the final calculation.

We obtained the relative importance (weight) of each structure in the total wave function Ψ :

$$\Psi = \sum_i c_i \Phi_i$$

from the VB-SCF calculation with all structures. The weights¹³ for each structure are calculated with

$$W_j = \sum_i c_i c_j S_{ij}$$

Furthermore, we wanted to get insight into the energy contributions of the structures to the total energy of the molecules. Because of the nonorthogonality of the structures in the valence-bond method the contributions of each of them and the resonances between them are not separable. We performed a Löwdin orthogonalization on the structures. Then the energy can be split into energy contributions for each structure (ϵ_i) and the resonances between them (ϵ_{ij}):¹⁴

$$E = \sum_i \sum_j c_i c_j H_{ij}^L = \sum_i c_i c_i H_{ii}^L + \sum_i \sum_{j>i} 2c_i c_j H_{ij}^L = \sum_i \epsilon_i + \sum_i \sum_{j>i} \epsilon_{ij}$$

In Figure 12 we show the orbitals that take part in the bonding of CpSiH; Figure 13 shows the orbitals for CpSiH₃. These orbital pictures are made with Molden.¹⁵ The contour surfaces are of orbital amplitude -0.1 (green) and 0.1 (blue).

Results

Approach. For a large number of cyclopentadienyl derivatives of groups 1, 2, and 11–15, we have calculated the most stable structures and—in many cases—relevant alternative structures. These are all listed in Table 1. For many species, Table 1 contains an η^2 structure as well as a $\sigma/\eta^1/\eta^3$ structure. Invariably, only *one* of these two is a local minimum, the other being the transition state for ring whizzing (movement of the metal atom along the periphery of the ring). The transition state was optimized by restriction to C_s symmetry, within which it is a local minimum.

For a selection of the species in Table 1, ring slippage potential energy curves have been determined. In ring

slippage curves calculated in this way for Cp₂M compounds, the *second* Cp ring will generally adjust its hapticity during the slippage, so that the “zero-slippage” point does *not* generally correspond to a $\eta^5:\eta^5$ structure. Where applicable, fully symmetric $D_{5d} \eta^5:\eta^5$ structures were calculated separately and are included in Table 1. Slippage curves are not intended to model the actual movement of the metal over the Cp ring. Rather, they are used to systematically explore the energies of the various bonding modes (central, peripheral, σ) of the metal fragment to the Cp ring.

From the slippage curves, we can obtain an impression of the region above the Cp ring that is accessible to the metal fragment within a given energy tolerance. This region can have different shapes, as illustrated in Figure 3. A *central* region includes the position above the ring centroid (though this does not necessarily correspond to the lowest energy). A *peripheral* region is obtained when the fragment can slip freely (within the given tolerance) along the ring perimeter but cannot move to the center. Finally, a *localized* region is obtained when only certain peripheral positions are accessible (e.g., only η^2 or only η^1). To quantify the flexibility of the system, we have calculated the shapes and areas (in Å²) of these regions for energy tolerances of 5 (A_5) and 10 (A_{10}) kcal/mol. The former tolerance is probably an upper limit to packing forces that could occur in a crystal, and hence the 5 kcal/mol region comprises the arrangements one could reasonably expect in the solid state. The 10 kcal/mol region represents the arrangements that are easily accessible at or somewhat below room temperature and could, for example, be frozen out in VT-NMR studies. For comparison, the total area of a cyclopentadienyl ring is approximately 7 Å². The results of the slippage curve calculations are summarized in Table 2.

In each of the sections below, we first describe the idealized structures obtained from the calculations on prototype compounds and then compare them to results of X-ray and electron-diffraction structure determinations. A perfect agreement cannot be expected, as (i) we have used only a moderate-size basis set for the calculations,^{1b} (ii) in view of the “floppiness” of many species, packing effects will have a large influence on the experimental structures, and (iii) for many cases, the prototype on which the calculations are performed is unknown or forms a polymer in the solid state, so that the comparison is with a more substituted derivative.

Nevertheless, the agreement between the calculated and observed structures is seen to be good enough that we feel justified in using the calculated structures and

(11) van Lenthe, J. H.; Balint-Kurti, G. G. *J. Chem. Phys.* **1983**, *78*, 5699–5713.

(12) van Lenthe, J. H.; Verbeek, J.; Pulay, P. *Mol. Phys.* **1991**, *73*, 1159–1170.

(13) Chirgwin, B. H.; Coulson, C. A. *Proc. R. Soc. London, Ser. A* **1950**, *201*, 196.

(14) Havenith, R. W. A.; van Lenthe, J. H.; Dijkstra, F.; Jennekens, L. W. *J. Phys. Chem. A* **2001**, *105*, 3838–3845.

(15) Schaftenaar, G.; Noordik, J. H. *J. Comput.-Aided Mol. Design* **2000**, *14*, 123–134.

Table 2. Slippage Curve Summaries

element	species	ϵ^b					A_5^c	A_{10}^c
		η^5^a	η^3^a	η^2^a	η^1^a	σ^a		
Li	CpLi	(0)	13	17	22	40	0.49 (c)	1.2 (c)
	Cp ₂ Li	(0)	3	4	5	12	4.6 (c)	15 (c)
Na	CpNa	(0)	6	8	11	24	1.5 (c)	4.0 (c)
	Cp ₂ Na	(0)	3	4	5	13	4.6 (c)	14 (c)
Be	CpBe ⁺	(0)	31	33	48	59	0.15 (c)	0.36 (c)
	CpBeH	(0)	14	18	21	32	0.44 (c)	1.1 (c)
	Cp ₂ Be	(0)	2	2	1	2	15 (c)	19 (c)
Mg	CpMg ⁺	(0)	11	13	17	26	0.52 (c)	1.6 (c)
	CpMgH	(0)	8	12	15	29	0.92 (c)	2.4 (c)
	Cp ₂ Mg	(0)	7	9	11	22	1.3 (c)	3.7 (c)
Cu	CpCu	(0)	2.5	2.5	3	8	8.5 (c)	16 (c)
	CpCu-PPh ₃	(0)	5	7	8	19	2.2 (c)	5.7 (c)
Ag	CpAg	5	3	2	1	3	18 (c)	25 (c)
	CpAg-PPh ₃	0	0	1	1	8	11 (c)	18 (c)
Au	CpAu	37	17	13	7	1	8.1 (l)	17 (p)
	CpAu-PPh ₃	11	4	4	2	2	13 (p)	21 (c)
Zn	CpZn ⁺	8	7	4	3	6	12 (p)	21 (c)
	CpZnH	(0)	4	6	7	17	2.7 (c)	6.8 (c)
	Cp ₂ Zn	1	0	0	0	5	15 (c)	21 (c)
Cd	CpCd ⁺	13	7	3	4	6	15 (p)	24 (p)
	CpCdH	(0)	2	4	5	15	4.4 (c)	10 (c)
	Cp ₂ Cd	0	0	0	0	5	15 (c)	23 (c)
Hg	CpHg ⁺	24	12	6	5	2	20 (p)	30 (p)
	CpHgH	4	0	1	0	6	14 (c)	21 (c)
B	CpBH ⁺	(0)	28	31	39	57	0.14 (c)	0.36 (c)
	CpBH ₂	39	11	4	3	5	8.7 (p)	14 (p)
	CpBCl ₂	65	25	12	11	(0)	5.3 (l)	12 (p)
	CpBMe ₂	50	20	10	8	1	8.9 (p)	14 (p)
	Cp ₂ B ⁺	(0)	19	27	15	(0)	19 (p/c)	36 (p/c)
Al	CpAl	(0)	9	13	16	32	0.92 (c)	2.2 (c)
	CpAlH ⁺	(0)	16	19	25	43	0.38 (c)	1.0 (c)
	CpAlH ₂	2	2	(0)	3	13	8.2 (c)	14 (c)
	CpAlH ₃ ⁻	16	8	7	4	1	11 (l)	24 (p)
Ga	Cp ₂ Al ⁺	(0)	8	9	11	17	0.99 (c)	4.1 (c)
	CpGa	(0)	8	11	14	30	1.2 (c)	2.7 (c)
	CpGaH ⁺	(0)	7	8	11	24	1.4 (c)	3.8 (c)
In	CpGaH ₂	10	4	1	2	10	9.5 (p)	17 (c)
	Cp ₂ Ga ⁺	(0)	2	2	1	2	17 (c)	21 (c)
	CpIn	(0)	7	10	13	30	1.4 (c)	3.2 (c)
	CpInH ⁺	(0)	4	6	8	19	2.6 (c)	6.8 (c)
Tl	CpInH ₂	5	2	(0)	2	10	11 (p)	18 (c)
	Cp ₂ In ⁺	0	1	2	1	2	19 (c)	24 (c)
	CpTl	(0)	7	9	12	30	1.6 (c)	3.6 (c)
	CpTlH ⁺	9	1	1	0	7	13 (p)	21 (c)
Si	CpTlH ₂	7	2	(0)	1	9	12 (p)	20 (c)
	Cp ₂ Tl ⁺ ^d	≈8	1	2	0	4	18 (p)	27 (c)
	CpSi ⁺	(0)	18	23	31	54	0.40 (c)	0.90 (c)
	CpSiH	15	2	(0)	4	15	6.4 (p)	12 (p)
Ge	CpSiH ₃	40	19	18	8	(0)	8.3 (l)	12 (l)
	CpGe ⁺	(0)	13	17	23	47	0.62 (c)	1.4 (c)
	CpGeH	13	2	(0)	3	15	7.3 (p)	12 (p)
Sn	CpGeH ₃	45	19	18	8	1	8.6 (l)	12 (l)
	CpSn ⁺	(0)	12	16	21	45	0.71 (c)	1.6 (c)
	CpSnH	8	2	(0)	3	16	8.2 (p)	14 (c)
Pb	CpSnH ₃	27	12	11	5	1	10 (l)	18 (p)
	CpPb ⁺	(0)	12	15	21	45	0.74 (c)	1.7 (c)
	CpPbH	7	3	(0)	1	16	8.2 (p)	14 (c)
As	CpPbH ₃	29	13	11	5	1	11 (l)	19 (p)
	CpAsH ⁺	28	8	(0)	7	24	3.5 (l)	9.5 (p)
Sb	CpAsH ₂	43	17	20	7	(0)	8.9 (l)	13 (l)
	CpSbH ⁺	18	5	1	5	21	6.3 (p)	12 (p)
Bi	CpSbH ₂	35	13	13	5	1	11 (l)	15 (l)
	CpBiH ⁺	14	3	0	4	22	7.4 (p)	12 (p)
Mn	CpBiH ₂	27	9	9	3	2	11 (l)	20 (p)
	CpMnH	(0)	9	12	16	35	0.99 (c)	2.3 (c)
	Cp ₂ Mn	(0)	6	8	11	25	1.8 (c)	4.6 (c)
Fe	CpMn(CO) ₃	(0)	23	32	39	72	0.26 (c)	0.61 (c)
	Cp ₂ Fe	(0)	28	36	45	74	0.20 (c)	0.49 (c)

^a Slippage assumed for selected arrangements: η^5 , 0 Å; η^3 , 0.8 Å; η^2 , 1.0 Å; η^1 , 1.2 Å. For σ the slip distance depends on the metal radius; the structure was optimized with $\angle\text{Cg}-\text{C}-\text{M}$ constrained to 125°. ^b Relative to lowest energy structure. ^c In Å². Area shapes: c = central, p = peripheral, l = local (see Figure 3). ^d On forcing an η^5 structure, Cp₂Tl⁺ collapses with a low barrier to a C-C coupled product.

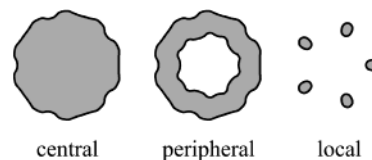


Figure 3. Shapes of accessible regions for movement of a metal fragment over a Cp ring.

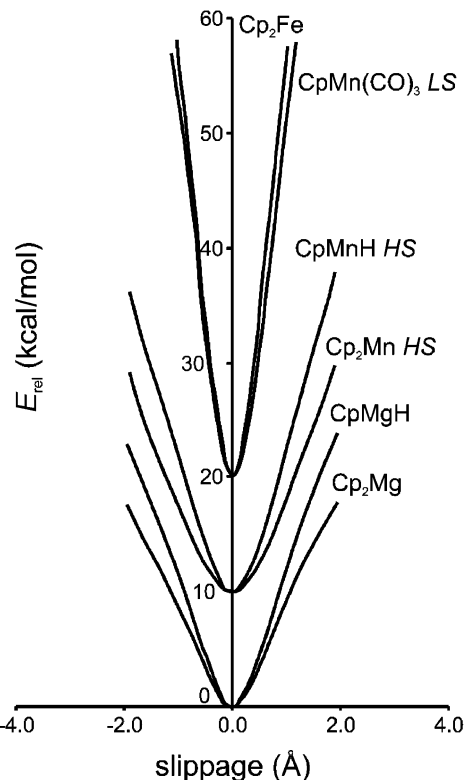


Figure 4. Slippage curves for Cp₂Mg, CpMgH, Cp₂Mn, CpMnH, CpMn(CO)₃, and Cp₂Fe. In this and the following figures, some of the curves are offset vertically for clarity.

energy profiles as a basis for the interpretation of structural preferences, in the Discussion part of the paper.

Groups 1 and 2. CpLi, Cp₂Li⁻, CpNa, Cp₂Na⁻, CpBe⁺, CpBeH, CpMg⁺, CpMgH, and Cp₂Mg all prefer η^5 structures, as expected for a mainly ionic^{1c,16} Cp–M interaction. The slippage curves are a bit softer for the larger elements Na and Mg, as would be expected on the basis of an electrostatic model (e.g. $A_5 = 0.49$ Å² for CpLi, 1.5 Å² for CpNa); slippage curves are also much softer for the dicyclopentadienyl systems than for the monocyclopentadienyl systems ($A_5 = 0.92$ Å² for CpMgH, 1.3 Å² for Cp₂Mg, 4.6 Å² for Cp₂Na⁻). Slippage curves for CpMgH and Cp₂Mg are shown in Figure 4 (a few iron and manganese derivatives are also included in the figure for reasons that will be explained later).

Monocyclopentadienyl derivatives of the group 1 elements are invariably associated and/or solvated,¹⁷

(16) Jemmis, E. D.; Schleyer, P. v. R. *J. Am. Chem. Soc.* **1982**, *104*, 4781. Waterman, K. C.; Streitwieser, A., Jr. *J. Am. Chem. Soc.* **1984**, *106*, 3138. Lambert, C.; Schleyer, P. v. R. *Angew. Chem.* **1994**, *106*, 1187.

(17) See e.g.: (a) Dinnebieer, R. E.; Behrens, U.; Olbrich, F. *Organometallics* **1997**, *16*, 3855 (CpLi, CpNa, and CpK); (b) Dohmeier, C.; Baum, E.; Ecker, A.; Köppe, R.; Schnöckel, H. *Organometallics* **1996**, *15*, 4702 (Bz₅C₅Li). (c) Jützi, P.; Leffers, W.; Hampel, B.; Pohl, S.; Saak, W. *Angew. Chem.* **1987**, *99*, 563 (Me₃SiC₅H₄K). (d) Hammel, A.;

which makes a comparison with the calculated structures difficult. The X-ray structures of the Cp_2Li^- and Cp_2Na^- ^{18,19} ions show approximately D_{5d} symmetric anions with metal–ring distances very similar to the ones we calculate; the agreement is a bit better than that obtained at the RHF level by Harder.^{19b} The X-ray structure of Cp_2Mg ²⁰ also shows a D_{5d} -symmetric structure, with a metal–ring distance slightly shorter (0.04 Å) than we calculate. The structure calculated for CpBeH shows fair agreement with that observed for CpBeMe in the gas phase;²¹ the structure of monomeric, gaseous $\text{CpMgCH}_2\text{tBu}$ ²² is also similar to the one we calculate for CpMgH .

The structure of Cp_2Be has been the subject of numerous experimental and theoretical investigations; the literature on this compound is extensive and will not be reviewed here.^{23,24} The X-ray structure shows an unusual slipped-sandwich structure.^{23a–c} Like others,^{1c,24d,f} we find that the minimum-energy structure has one η^5 -bound and one η^1 -bound ring. Thus, the two “minima” along the Cp_2Be slippage curve in Figure 5 actually represent the same structure. There is a low barrier (1.8 kcal/mol) for exchange of the rings via a η^3 : η^3 structure. The avoidance of a η^5 : η^5 structure (which is ca. 2 kcal/mol above the η^5 : η^1 minimum) has been interpreted as evidence for covalency (with its concomitant preference for electron-precise structures) or as a consequence of excessive steric repulsion between the two rings in the η^5 : η^5 structure due to the small radius of Be. Presumably, both effects are important; we will return to this point later. Provided that the second Cp ring is allowed to adjust its hapticity, movement of the Be atom over the whole area of the first Cp ring is nearly

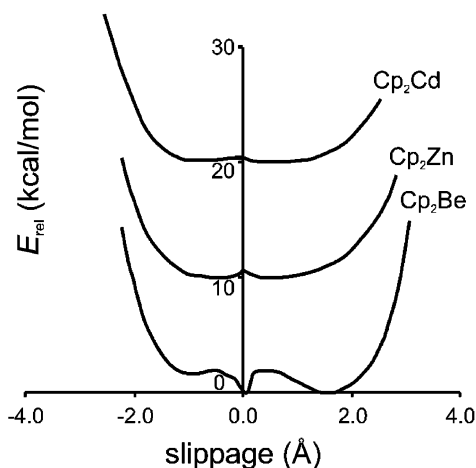


Figure 5. Slippage curves for Cp_2Be , Cp_2Zn , and Cp_2Cd .

free (within 2 kcal/mol). The accessible area A_5 is 15 Å², i.e., more than twice the area of the Cp ring itself! Of the substituted beryllocenes, $(\text{Me}_4\text{C}_5\text{H}_2)\text{Be}$ has been found to have a slip-sandwich structure similar to Cp_2Be , but the even more crowded $(\text{Me}_5\text{C}_5)_2\text{Be}$ surprisingly has a structure that is closer to η^5 : η^5 .²⁵

Group 11. While normally considered to be transition metals, the elements Cu–Au have been included here because their metal(I) cyclopentadienyls, having a completely filled d shell, are more reminiscent of main-group-metal derivatives. Of the formally 16e uncomplexed CpM species, CpCu has a soft slippage mode ($A_5 = 8.5$ Å²) with a weak preference for η^5 bonding, while CpAg has an even softer slippage mode ($A_5 = 18$ Å²) mode, but now with a weak preference for η^1 bonding (see Figure 6 for geometries along the path), and CpAu is clearly σ -bound. Adding a phosphine ligand, to form an 18e $\text{CpM}\cdot\text{PH}_3$ complex, results in an increased tendency toward polyhapt bonding: CpCu $\cdot\text{PH}_3$ is strongly η^5 -bound ($A_5 = 2.2$ Å²), CpAg $\cdot\text{PH}_3$ has a weak preference for η^5 bonding ($A_5 = 11$ Å²), and although CpAu $\cdot\text{PH}_3$ is σ -bound the difference with the η^5 -bound structure has become smaller than for uncomplexed CpAu. Thus, increasing saturation of the metal does not necessarily result in a decreased tendency for η^5 bonding!

Experimentally, ligand-free Cp–group 11 complexes are unknown. CpCu $\cdot\text{PR}_3$ complexes are generally η^5 -bound,²⁶ although the interaction has been stated to be weaker than usually observed for transition metals.^{26d} The X-ray structure of $(\text{Me}_3\text{Si})_3\text{C}_5\text{H}_2\text{Ag}\cdot\text{P}n\text{Bu}_3$ contains two independent molecules, which are approximately η^3 and η^4 bound.²⁷ Complexes of the type CpAu $\cdot\text{PR}_3$ are consistently η^1 -bound.²⁸

Group 12. The group 12 systems are clearly more “floppy” than the corresponding group 2 systems (e.g.

Schwarz, W.; Weidlen, K. *Acta Crystallogr.* **1990**, *C46*, 2337 ($\text{MeC}_5\text{H}_4\text{Li}\cdot\text{pmdta}$). (e) Jützi, P.; Schlüter, E.; Krüger, C.; Pohl, S. *Angew. Chem.* **1983**, *95*, 1015 ($(\text{Me}_3\text{Si})_3\text{C}_5\text{H}_2\text{Li}\cdot\text{pmdta}$). (f) Jützi, P.; Leffers, W.; Pohl, S.; Saak, W. *Chem. Ber.* **1989**, *122*, 1449 ($(\text{Me}_3\text{Si})_3\text{C}_5\text{H}_2\text{Li}\cdot\text{THF}$). (g) Jützi, P.; Schlüter, E.; Pohl, S.; Sak, W. *Chem. Ber.* **1985**, *118*, 1959 ($(\text{Me}_3\text{Si})_3\text{C}_5\text{H}_2\text{Li}\cdot\text{L}$, L = tmeda, quinuclidine). (h) Lappert, M. F.; Singh, A.; Engelhardt, L. M.; White, A. H. *J. Organomet. Chem.* **1984**, *262*, 271 ($\text{Me}_3\text{SiC}_5\text{H}_4\text{Li}\cdot\text{tmeda}$). (i) Aoyagi, T.; Shearer, H. M. M.; Wade, K.; Whitehead, G. *J. Chem. Soc., Chem. Commun.* **1976**, 164 ($\text{CpNa}\cdot\text{tmeda}$). (j) Rabe, G.; Roesky, H. W.; Stalke, D.; Pauer, F.; Sheldrick, G. M. *J. Organomet. Chem.* **1991**, *403*, 11 ($\text{Me}_3\text{C}_5\text{Na}\cdot 3$ Py, $\text{CpK}\cdot 2$ Py). (k) Edelman, M. A.; Hitchcock, P. B.; Lappert, M. F.; Liu, D.-S.; Tian, S. *J. Organomet. Chem.* **1998**, *550*, 397 ($(\text{Me}_3\text{Si})_3\text{C}_5\text{H}_2\text{Na}\cdot\text{pmdta}$). (l) Lorberth, J.; Shin, S.-H.; Wocadlo, S.; Massa, W. *Angew. Chem.* **1989**, *101*, 793 ($\text{Bz}_5\text{C}_5\text{K}\cdot 2\text{THF}$).

(18) Wessel, J.; Lork, E.; Mews, R. *Angew. Chem.* **1995**, *107*, 2565.
 (19) (a) Harder, S.; Proscenc, M. H. *Angew. Chem.* **1994**, *106*, 1830.
 (b) Harder, S.; Proscenc, M. H.; Rief, U. *Organometallics* **1996**, *15*, 118.
 (20) Bündler, W.; Weiss, E. *J. Organomet. Chem.* **1975**, *92*, 1.
 (21) Drew, D. A.; Haaland, A. *Acta Chem. Scand.* **1972**, *26*, 3079.
 (22) Andersen, R. A.; Blom, R.; Haaland, A.; Schilling, B. E. R.; Volden, H. V. *Acta Chem. Scand.* **1985**, *A39*, 563.
 (23) X-ray structures: (a) Wong, C.-H.; Lee, T.-Y.; Chao, K.-J.; Lee, S. *Acta Crystallogr.* **1972**, *B28*, 1662. (b) Wong, C.; Lee, T. Y.; Chang, T. W.; Liu, C. S. *Inorg. Nucl. Chem. Lett.* **1973**, *9*, 667. (c) Nugent, K. W.; Beattie, J. K.; Hambley, T. W.; Snow, M. R. *Aust. J. Chem.* **1984**, *37*, 1601. Electron diffraction studies: (d) Haaland, A. *Acta Chem. Scand.* **1968**, *22*, 3030. (e) Almenningen, A.; Haaland, A.; Luszyk, J. *J. Organomet. Chem.* **1979**, *170*, 271. IR: (f) Nugent, K. W.; Beattie, J. K. *Inorg. Chem.* **1988**, *27*, 4269. Microwave: (g) Pratten, S. J.; Cooper, M. K.; Aroney, M. J.; Filipczuk, S. W. *J. Chem. Soc., Dalton Trans.* **1985**, 1761. NMR: (h) Nugent, K. W.; Beattie, J. K. *J. Chem. Soc., Chem. Commun.* **1986**, 186. (i) Pratten, S. J.; Cooper, M. K.; Aroney, M. J. *J. Organomet. Chem.* **1990**, *381*, 147.

(24) (a) Jemmis, E. D.; Alexandratos, S.; Schleyer, P. v. R.; Streitwieser, A., Jr.; Schafer, H. F., III. *J. Am. Chem. Soc.* **1978**, *100*, 5695. (b) Gribov, L. A.; Raikhstat, M. M.; Zhogina, V. V. *Koord. Khim.* **1988**, *14*, 1368. (c) Beattie, J. K.; Nugent, K. W. *Inorg. Chim. Acta* **1992**, *198*, 309. (d) Margl, P.; Schwarz, K.; Blöchl, P. E. *J. Am. Chem. Soc.* **1994**, *116*, 11177. (e) Margl, P.; Schwarz, K.; Blöchl, P. E. *J. Chem. Phys.* **1995**, *103*, 683. (f) Mire, L. S.; Wheeler, S. D.; Wagenscheller, E.; Marynick, D. S. *Inorg. Chem.* **1998**, *37*, 3099.

(25) Conejo, M. M.; Fernández, R.; Gutiérrez-Puebla, E.; Monge, Á.; Ruiz, C.; Carmona, E. *Angew. Chem., Int. Ed.* **2000**, *39*, 1949.

(26) (a) Cotton, F. A.; Takats, J. *J. Am. Chem. Soc.* **1970**, *92*, 2353. (b) Delbaere, L. T. J.; McBride, D. W.; Ferguson, R. B. *Acta Crystallogr.* **1970**, *B26*, 515. (c) Hanusa, T. P.; Ullbarri, T. A.; Evans, W. J. *Acta Crystallogr.* **1985**, *C41*, 1036. (d) Anderson, Q. T.; Erkizia, E.; Conry, R. R. *Organometallics* **1998**, *17*, 4917. (e) Cotton, F. A.; Marks, T. J. *J. Am. Chem. Soc.* **1969**, *91*, 7281.

(27) Stämmler, H.-G.; Jützi, P.; Wieland, W. *Acta Crystallogr.* **1998**, *C54*, 64.

(28) (a) Werner, H.; Otto, H.; Ngo-Khac, T.; Burschka, C. *J. Organomet. Chem.* **1984**, *262*, 123. (b) Baukova, T. V.; Slovokhotov, Y. L.; Struchkov, Y. T. *J. Organomet. Chem.* **1981**, *220*, 125. (c) Ortaggi, G. *J. Organomet. Chem.* **1974**, *80*, 275.

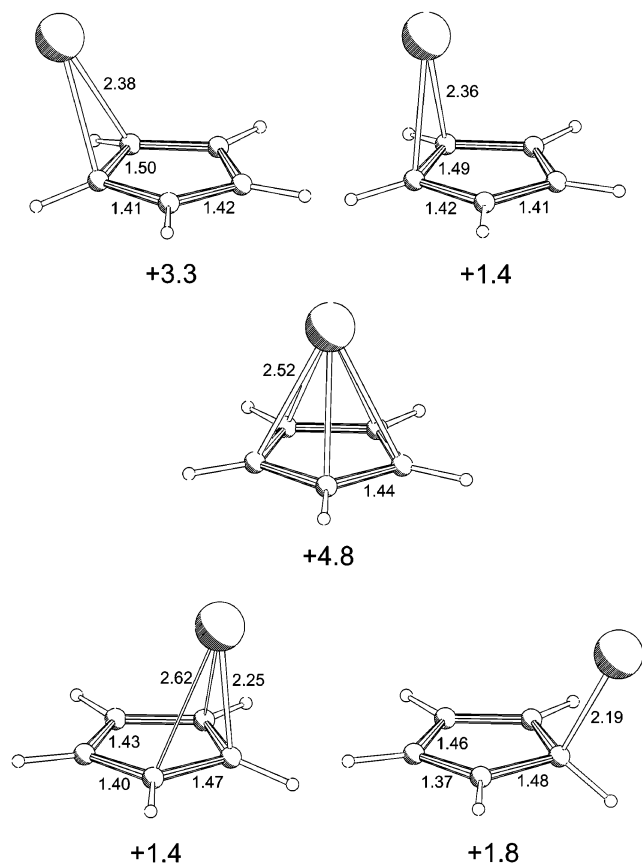


Figure 6. Representative geometries along the slippage curve of CpAg. Distances are given in Å and relative energies in kcal/mol.

CpMgH, $A_5 = 0.92 \text{ \AA}^2$; CpZnH, $A_5 = 2.7 \text{ \AA}^2$). CpZnH and CpCdH prefer η^5 -bound structures, while CpHgH has a σ -bound structure. Similarly, Cp₂Zn and Cp₂Cd are $\eta^3:\eta^3$ bound, while Cp₂Hg is $\sigma:\sigma$. The electron-excess D_{5d} structure is weakly avoided in Cp₂Zn and Cp₂Cd (by less than 1 kcal/mol), but is strongly destabilized for Cp₂Hg (23 kcal/mol higher than $\sigma:\sigma$). For the cations CpM⁺, we see a clear preference for more localized bonding, which increases from Zn to Hg. Thus, we again find the counterintuitive tendency that increasing the metal saturation (going from CpM⁺ to CpMH) leads to higher hapticity. CpZnH₂⁻, the model for a Lewis base adduct of CpZnH, prefers an η^2 structure similar to that of CpAlH₂ (see below).

The “metallocenes” Cp₂Zn and Cp₂Cd are subtly different from Cp₂Be (see Figure 5). Whereas beryllocene prefers the $\eta^3:\eta^1$ structure and has a small barrier to ring exchange via a $\eta^3:\eta^3$ structure, we find that Cp₂Zn and Cp₂Cd actually prefer the $\eta^3:\eta^3$ structure, the $\eta^5:\eta^1$ structure being ca. 0.5 kcal/mol higher in energy. Rayón and Frenking, using a different functional and basis set, report a preference of Cp₂Zn for a $\eta^5:\eta^1$ structure.^{1c} In any case, for all three compounds movement over all of the ring area is virtually free. Geometries for some representative points along the slippage curve of Cp₂Zn are shown in Figure 8. The extreme ease of the slippage in Cp₂Zn and Cp₂Cd is reflected by their A_5 values of 15 Å². In view of the much larger sizes of Zn and Cd compared to Be, the preference for an electron-precise structure must now be caused by covalency rather than by steric effects.

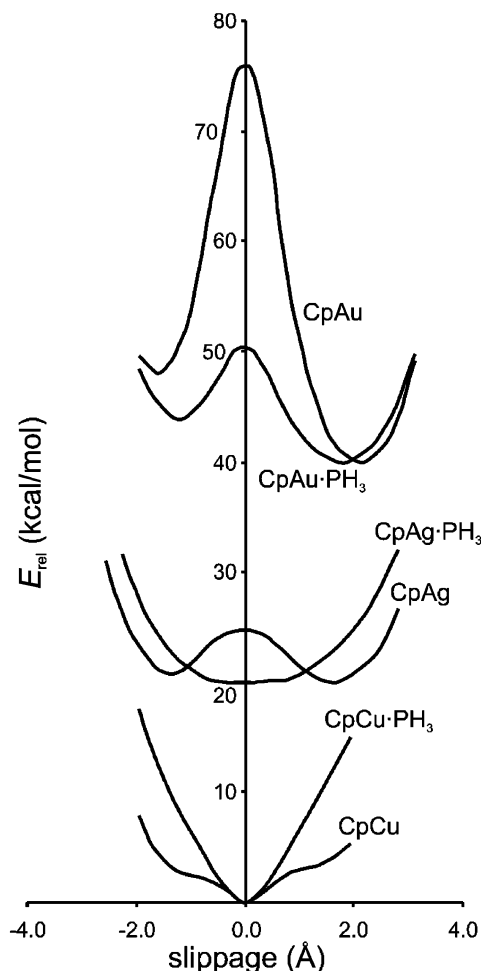


Figure 7. Slippage curves for CpCu, CpAg, CpAu, and their PH₃ complexes.

Experimentally, monomeric CpZnX compounds have an η^5 -bound Cp ring.²⁹ The structure of monomeric Cp₂Zn is unknown (in the solid state it is a polymer³⁰); the monomeric substituted derivatives (Me₅C₅)₂Zn,^{31a-c} (PhMe₄C₅)₂Zn,^{31c} (tPr₄C₅)₂Zn,^{31d} and (Me₃SiC₅H₄)₂Zn^{31c} all appear to adopt the “slipped-sandwich” $\eta^5:\eta^1$ structure instead of the $\eta^3:\eta^3$ structure we calculate for the parent compound. The structure of base-free Cp₂Cd is unknown; the Cp groups are η^1 -bound in Cp₂Cd-(Py)₂^{32a} and Cp₂Cd-(pmdta)^{32b} but η^2 -bound in Cp₂Cd-(tmeda).^{32b} Cyclopentadienyl derivatives of mercury appear to be σ -bound;^{26e} in the case of Cp₂Hg,^{33a} (tBu₃C₅H₂)₂Hg,^{33b} (tBuSiMe₂Me₄C₅)₂Hg,^{33c} (tBuSiMe₂-

(29) (a) Haaland, A.; Samdal, S.; Seip, R. *J. Organomet. Chem.* **1978**, *153*, 187. (b) Budzelaar, P. H. M.; Boersma, J.; Van der Kerk, G. J. M.; Spek, A. L.; Duisenberg, A. J. M. *Inorg. Chem.* **1982**, *21*, 3777. (c) Budzelaar, P. H. M.; Den Haan, K. H.; Boersma, J.; Van der Kerk, G. J. M.; Spek, A. L. *Organometallics* **1984**, *3*, 156. (d) Budzelaar, P. H. M.; Van der Zeijden, A. A. H.; Boersma, J.; Van der Kerk, G. J. M.; Spek, A. L.; Duisenberg, A. J. M. *Organometallics* **1984**, *3*, 159.

(30) Budzelaar, P. H. M.; Boersma, J.; Van der Kerk, G. J. M.; Spek, A. L.; Duisenberg, A. J. M. *J. Organomet. Chem.* **1985**, *281*, 123.

(31) (a) Blom, R.; Haaland, A.; Weidlein, J. *J. Chem. Soc., Chem. Commun.* **1985**, 266. (b) Blom, R.; Boersma, J.; Budzelaar, P. H. M.; Fischer, B.; Haaland, A.; Volden, H. V.; Weidlein, J. *Acta Chem. Scand.* **1986**, *A40*, 113. (c) Fischer, B.; Wijkens, P.; Boersma, J.; Van Koten, G.; Smeets, W. J. J.; Spek, A. L.; Budzelaar, P. H. M. *J. Organomet. Chem.* **1989**, *376*, 223. (d) Burkey, D. J.; Hanusa, T. P. *J. Organomet. Chem.* **1996**, *512*, 165.

(32) (a) Smeets, W. J. J.; Spek, A. L.; Fischer, B.; Van Mier, G. P. M. *Acta Crystallogr.* **1987**, *C43*, 893. (b) Barr, D.; Edwards, A. J.; Raithby, P. R.; Rennie, M.-A.; Verhorevoort, K. L.; Wright, D. S. *J. Organomet. Chem.* **1995**, *493*, 175.

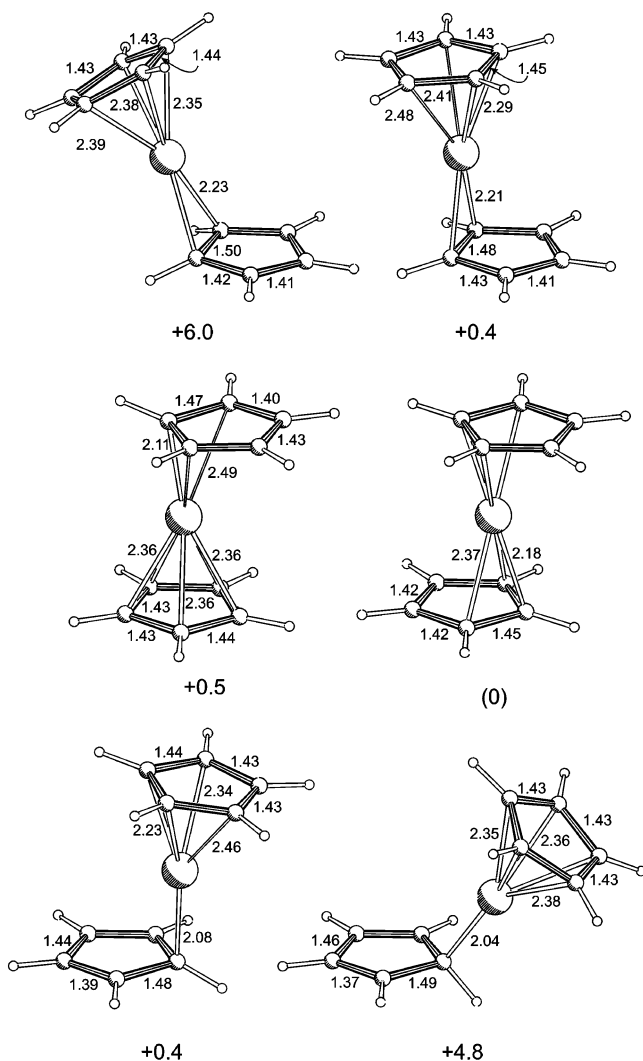


Figure 8. Representative geometries along the slippage curve of Cp_2Zn . Distances are given in Å and relative energies in kcal/mol.

$\text{Me}_4\text{C}_5\text{HgCl}$,^{33c} and $\text{Cl}_5\text{C}_5\text{HgPh}$,^{33d} this has been confirmed by X-ray diffraction.

Group 13. The metal(I) cyclopentadienyls of Al–Tl all prefer η^5 -bound structures with rather long M–Cp bonds. However, deformation toward lower hapticity is not particularly easy, as illustrated by the similarity of the A_5 values for CpAl and CpMgH (both 0.92 \AA^2). This demonstrates that the large Cp–M distance does not imply a weak bond. On formal protonation of the metal lone pair, to give CpMH^+ , the metal–ring distance decreases, but—especially for the heavier group 13 elements—the preference for η^5 bonding also decreases (e.g., $A_5 = 1.4 \text{ \AA}^2$ for CpIn, 2.6 \AA^2 for CpInH⁺). In fact, CpTlH⁺ prefers an η^1 structure. In the series of dicyclopentadienyl derivatives Cp_2M^+ , we find a curious alternation of structural types, which has in part (B, Al, Ga) already been reported by Cowley.² Cp_2B^+ strongly prefers an electron-precise $\eta^5:\eta^1$ structure,

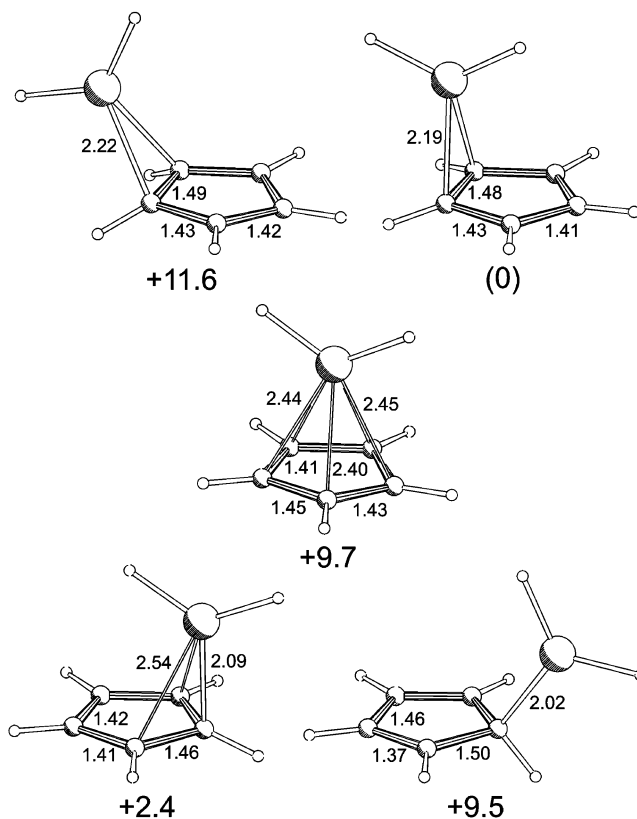


Figure 9. Representative geometries along the slippage curve of CpGaH_2 . Distances are given in Å and relative energies in kcal/mol.

similar to Cp_2Be but even more compact. Cp_2Al^+ has a $\eta^5:\eta^5$ D_{5d} structure similar to Cp_2Mg . Cp_2Ga^+ and Cp_2In^+ both again have a $\eta^5:\eta^1$ structure, with the electron-excess D_{5d} structure ca. 7 kcal/mol higher in energy. Cp_2Tl^+ has a $\eta^1:\eta^1$ structure, and here, as for Cp_2Hg , the D_{5d} structure is strongly avoided (by 44 kcal/mol). According to our calculations, Cp_2Tl^+ easily collapses to a C–C coupled structure; therefore, we think that isolation of unsubstituted Cp_2Tl^+ derivatives is unlikely.

The neutral complexes CpMH_2 ($M = \text{B–Tl}$) all prefer η^2 -bound structures, although the energy difference with the η^3 (or η^1) isomer is uniformly small (1–2.5 kcal/mol). The central η^5 -bound structure is strongly avoided for $M = \text{B}$ and weakly avoided for $M = \text{Ga–Tl}$ (by 5–10 kcal/mol), whereas for Al slippage of the MH_2 fragment over all of the ring area is nearly free (within ~ 2 kcal/mol). Geometries for some representative points along the slippage curve of CpGaH_2 are shown in Figure 9.

In the series of dicyclopentadienyl hydrides Cp_2MH , Al prefers a $\eta^2:\eta^2$ structure (Al–C bond lengths of 2.15 and 2.20 Å), whereas with the heavier congeners Ga–Tl the situation is better described as $\eta^{1.5}:\eta^{1.5}$ (e.g., Ga–C bond lengths of 2.13 and 2.34 Å). CpAlH_3^- , as a model for a Lewis base adduct of CpAlH_2 , prefers the expected σ -bound structure.

Substituents can also influence the preferred coordination mode: whereas CpBH_2 favors an η^2 -bound structure by 2.0 kcal/mol, the σ -bound structure is preferred for CpBMe_2 (by 3.7 kcal/mol) and CpBCl_2 (by 5.9 kcal/mol). One would expect stronger π -donors than Cl (e.g. alkoxides or amides) to induce an even larger preference for σ - CpBX_2 structures. For aluminum, the effects of substituents are different: going from CpAlH_2

(33) (a) Fischer, B.; Van Mier, G. P. M.; Boersma, J.; Van Koten, G.; Smeets, W. J. J.; Spek, A. L. *Recl. Trav. Chim. Pays-Bas* **1988**, *107*, 259. (b) Sitzmann, H.; Wolmershäuser, G. *Z. Anorg. Allg. Chem.* **1995**, *621*, 109. (c) Hitchcock, P. B.; Keates, J. M.; Lawless, G. A. *J. Am. Chem. Soc.* **1998**, *120*, 599. (d) Davies, A. G.; Goddard, J. P.; Hursthouse, M. B.; Walker, N. P. C. *J. Chem. Soc., Dalton Trans.* **1985**, 471.

to CpAlMe₂ increases the preference for the η^2 structure (over η^3) from 1.6 to 2.4 kcal/mol; CpAlCl₂ prefers an η^5 structure. Going from CpAlH₃⁻ to CpAlCl₃⁻ somewhat unexpectedly increases the preference for a σ -bound structure from 5.1 to 7.4 kcal/mol.

Uncomplexed cyclopentadienylboron(I) compounds are unknown. CpAl, generated at low temperature in solution, appears to form a tetramer; at higher temperatures it decomposes.^{34a} Me₅C₅Al is more stable. In solution the monomer is in equilibrium with the tetramer;^{34a} in the gas phase the monomer has an Al–Cp distance of 2.06 Å,^{34b} equal to the one we calculate for CpAl, while the tetramer observed in the solid state has somewhat shorter Al–Cp distances.^{34c} Monomeric CpGa is also unstable.^{35a} Me₅C₅Ga forms a curious hexameric structure in the solid state,^{35b} but in the gas phase it is monomeric like the Al analogue, with a metal–ring distance of 2.08 Å^{35c} (calcd for CpGa 2.18 Å). Many cyclopentadienyl derivatives of indium(I)³⁶ and thallium(I)^{36a,37} have been reported. They invariably have η^5 -bound Cp rings and usually form polymers in the solid state through either Cp bridging or metal–metal interactions (the latter presumably being rather weak³⁸). Me₄(Ph₂P)C₅In is monomeric in the solid state, with a ring–centroid distance of 2.41 Å.^{36h} In the gas phase, CpIn,^{36d} MeC₅H₄In,^{36d} and Me₅C₅In^{36e} have metal–ring distances of 2.32, 2.31, and 2.29 Å, respectively (calcd for CpIn 2.36 Å); in the solid state, Me₅C₅In forms hexamers with a ring–metal distance of 2.30

(34) (a) Gauss, J.; Schneider, U.; Ahlrichs, R.; Dohmeier, C.; Schnöckel, H. *J. Am. Chem. Soc.* **1993**, *115*, 2402. (b) Haaland, A.; Martinsen, K.-G.; Shlykov, S. A.; Volden, H. V.; Dohmeier, C.; Schnöckel, H. *Organometallics* **1995**, *14*, 3116. (c) Dohmeier, C.; Robl, C.; Tacke, M.; Schnöckel, H. *Angew. Chem.* **1991**, *103*, 594.

(35) (a) Loos, D.; Schnöckel, H.; Gauss, J.; Schneider, U. *Angew. Chem.* **1992**, *104*, 1376. (b) Loos, D.; Baum, E.; Ecker, A.; Schnöckel, H.; Downs, A. *J. Angew. Chem.* **1997**, *109*, 894. (c) Haaland, A.; Martinsen, K.-G.; Volden, H. V.; Loos, D.; Schnöckel, H. *Acta Chem. Scand.* **1994**, *48*, 172.

(36) (a) Frasson, E.; Menegus, F.; Panattoni, C. *Nature (London)* **1963**, *199*, 1087 (CpIn). (b) Beachley, O. T., Jr.; Churchill, M. R.; Fettinger, J. C.; Pazik, J. C.; Victoriano, L. *J. Am. Chem. Soc.* **1986**, *108*, 4666 (Me₅C₅In). (c) Jutzi, P.; Leffers, W.; Müller, G. *J. Organomet. Chem.* **1987**, *334*, 1987 ((Me₃Si)₂C₅H₄In). (d) Beachley, O. T., Jr.; Pazik, J. C.; Glassman, T. E.; Churchill, M. R.; Fettinger, J. C.; Blom, R. *Organometallics* **1988**, *7*, 1051 (CpIn, MeC₅H₄In). (e) Beachley, O. T., Jr.; Blom, R.; Churchill, M. R.; Fægri, K., Jr.; Fettinger, J. C.; Pazik, J. C.; Victoriano, L. *Organometallics* **1989**, *8*, 346 (Me₅C₅In). (f) Schumann, H.; Janiak, C.; Görlitz, F.; Loebel, J.; Dietrich, A. *J. Organomet. Chem.* **1989**, *363*, 243 (Bz₅C₅In). (g) Beachley, O. T., Jr.; Lees, J. F.; Rogers, R. D. *J. Organomet. Chem.* **1991**, *418*, 165 (tBuC₅H₄In). (h) Schumann, H.; Ghodsi, T.; Esser, L. *Acta Crystallogr.* **1992**, *C48*, 618 (Me₄(Ph₂P)C₅In).

(37) (a) Tyler, J. K.; Cox, A. P.; Sheridan, J. *Nature* **1959**, *183*, 1182 (CpTl). (b) Berar, J. F.; Calvarin, G.; Pommier, C.; Weigel, D. *J. Appl. Crystallogr.* **1975**, *8*, 386 (CpTl). (c) Freeman, M. B.; Sneed, L. G.; Huffman, J. C. *J. Am. Chem. Soc.* **1977**, *99*, 5194 ((NC)₂C=C(CN)-C₅H₄Tl). (d) Werner, H.; Otto, H.; Kraus, H. *J. Organomet. Chem.* **1986**, *315*, C57 (Me₅C₅Tl). (e) Schumann, H.; Janiak, C.; Pickardt, J.; Börner, U. *Angew. Chem.* **1987**, *99*, 788 (Bz₅C₅Tl). (f) Harvey, S.; Raston, C. L.; Skelton, B. W.; White, A. H.; Lappert, M. F.; Srivastava, G. *J. Organomet. Chem.* **1987**, *328*, C1 (Me₃SiC₅H₄Tl, (Me₃Si)₂C₅H₃Tl). (g) Schumann, H.; Janiak, C.; Khan, M. A.; Zuckerman, J. J. *J. Organomet. Chem.* **1988**, *354*, 7 (Bz₅C₅Tl). (h) Blom, R.; Werner, H.; Wolf, J. *J. Organomet. Chem.* **1988**, *354*, 293 (Me₅C₅Tl). (i) Schumann, H.; Kucht, H.; Dietrich, A.; Esser, L. *Chem. Ber.* **1990**, *123*, 1811 (Me₄(PhSiMe₂)C₅Tl, Me₄(PhCH₂SiMe₂)C₅Tl). (j) Jutzi, P.; Schnittger, J.; Hursthouse, M. B. *Chem. Ber.* **1991**, *124*, 1693 (tBu₄C₁₀H₄Tl₂). (k) Schumann, H.; Ghodsi, T.; Esser, L.; Hahn, E. *Chem. Ber.* **1993**, *126*, 591 (Me₄(Ph₂P)C₅Tl). (l) Frank, W.; Kuhn, D.; Müller-Becker, S.; Razavi, A. *Angew. Chem.* **1993**, *105*, 102 (FluCM₂C₅H₄Tl). (m) Schumann, H.; Lentz, A.; Weimann, R. *J. Organomet. Chem.* **1995**, *487*, 245 (Ph₂C₅H₃Tl). (n) Sawamura, M.; Iikura, H.; Nakamura, E. *J. Am. Chem. Soc.* **1996**, *118*, 12850 (Ph₃C₆₀Tl-THF).

(38) Janiak, C.; Hoffmann, R. *Angew. Chem.* **1989**, *101*, 1706. Budzelaar, P. H. M.; Boersma, J. *Recl. Trav. Chim. Pays-Bas* **1990**, *109*, 187. Schwerdtfeger, P. *Inorg. Chem.* **1991**, *30*, 1660.

Å.^{36b,e} Thallium complexes which are monomeric in the solid state include Me₄(Ph₂P)C₅Tl (2.51 Å),^{37k} Ph₅C₆₀-Tl(THF) (2.60 Å),³⁷ⁿ and one of the two modifications of Bz₅C₅Tl (2.49 Å).^{37h} In the gas phase, CpTl^{37a} and Me₅C₅Tl³⁷ⁱ have metal–ring distances of 2.41 and 2.37 Å (cf. 2.52 Å calcd for CpTl). Me₅C₅M¹ compounds (M = B–In) are versatile terminal and bridging 2e donors for main-group and transition metals, and in the resulting complexes the Me₅C₅ ring is consistently η^5 -bound, with a metal–ring distance that is shortened relative to uncomplexed Me₅C₅M.³⁹

Monocyclopentadienyl cations CpMX⁺ of the group 13 metals are only known for M = B. All examples reported to date have an η^5 -bound Cp group (*nido*-carborane structure).⁴⁰ Of the Cp₂M⁺ species, (Me₅C₅)₂B⁺ has the expected η^5 : η^1 structure,^{40b,e} (Me₅C₅)₂Al⁺ has a η^5 : η^5 structure,^{42h,n,o} and [(Me₅C₅)₂GaBF₄]₂ has a η^3 : η^1 structure. In the last case, the deviation of the polyhaptobound Cp ring from the nearly ideal η^5 arrangement calculated for Cp₂Ga⁺ may be caused by interaction of the Ga centers with the BF₄ groups;² since in the X-ray structure the η^1 -bound ring is slipped *less* than calculated for the isolated cation, the distortion may be viewed not so much as a reduction of hapticity but rather as a deformation toward a η^3 : η^3 arrangement.

There are no X-ray structures of cyclopentadienylboron dihydrides, dialkyls, or dihalides; the closest relative is probably Me₅C₅B(Cl)(As^tBu₂), which has the expected σ -bound structure.⁴¹ CpAlMe₂ forms a coordination polymer with bridging Cp groups in the solid state.^{42b} In the gas phase, the Cp ring is bound in a *polyhapt*o fashion, presumably η^2 .^{42a} CpMX₂ derivatives

(39) (a) Cowley, A. H.; Lomeli, V.; Voigt, A. *J. Am. Chem. Soc.* **1998**, *120*, 6401. (b) Greiwe, P.; Bethausler, A.; Pritzkow, H.; Kuhler, T.; Jutzi, P.; Siebert, W. *Eur. J. Inorg. Chem.* **2000**, *9*, 1927. (c) Dohmeier, C.; Krautscheid, H.; Schnöckel, H. *Angew. Chem.* **1994**, *106*, 2570. (d) Weiss, J.; Stetzkamp, D.; Nuber, B.; Fischer, R. A.; Boehme, C.; Frenking, G. *Angew. Chem.* **1997**, *109*, 95. (e) Üffing, C.; Ecker, A.; Köppe, R.; Schnöckel, H. *Organometallics* **1998**, *17*, 2373. (f) Gorden, J. D.; Voigt, A.; Macdonald, C. L. B.; Silverman, J. S.; Cowley, A. H. *J. Am. Chem. Soc.* **2000**, *122*, 950. (g) Weiss, D.; Steinke, T.; Winter, M.; Fischer, R. A.; Fröhlich, N.; Uddin, J.; Frenking, G. *Organometallics* **2000**, *19*, 4583. (h) Jutzi, P.; Neumann, B.; Reumann, G.; Stammer, H.-G. *Organometallics* **1998**, *17*, 1305. (i) Jutzi, P.; Neumann, B.; Schebaum, L. O.; Stammer, A.; Stammer, H.-G. *Organometallics* **1999**, *18*, 4462. (j) Jutzi, P.; Neumann, B.; Schebaum, L. O.; Stammer, A.; Stammer, H.-G. *Organometallics* **2000**, *19*, 1445. (k) Jutzi, P.; Neumann, B.; Reumann, G.; Schebaum, L. O.; Stammer, H.-G. *Organometallics* **1999**, *18*, 2550.

(40) (a) Jutzi, P.; Seufert, A. *Angew. Chem.* **1977**, *89*, 339. (b) Jutzi, P.; Seufert, A. *J. Organomet. Chem.* **1978**, *161*, C5. (c) Dohmeier, C.; Köppe, R.; Robl, C.; Schnöckel, H. *J. Organomet. Chem.* **1995**, *487*, 127. (d) Holtmann, U.; Jutzi, P.; Kühler, T.; Neumann, B.; Stammer, H.-G. *Organometallics* **1999**, *18*, 5531. (e) Voigt, A.; Filippini, S.; Macdonald, C. L. B.; Gorden, J. D.; Cowley, A. H. *Chem. Commun.* **2000**, 911.

(41) Petrie, M. A.; Olmstead, M. M.; Hope, H.; Bartlett, R. A.; Power, P. P. *J. Am. Chem. Soc.* **1993**, *115*, 3221.

(42) (a) Drew, D. A.; Haaland, A. *J. Chem. Soc., Chem. Commun.* **1972**, 1300. (b) Teclé, B.; Corfield, P. W. R.; Oliver, J. P. *Inorg. Chem.* **1982**, *21*, 458. (c) Fisher, J. D.; Shapiro, P. J.; Yap, G. P. A.; Rheingold, A. L. *Inorg. Chem.* **1996**, *35*, 271. (d) Fisher, J. D.; Shapiro, P. J.; Budzelaar, P. H. M.; Staples, R. J. *Inorg. Chem.* **1998**, *37*, 1295. (e) Dohmeier, C.; Schnöckel, H.; Robl, C.; Schneider, U.; Ahlrichs, R. *Angew. Chem.* **1994**, *106*, 225. (f) Schulz, S.; Häming, L.; Herbst-Irmer, R.; Roesky, H. W.; Sheldrick, G. M. *Angew. Chem.* **1994**, *106*, 1052. (g) Schulz, S.; Voigt, A.; Roesky, H. W.; Häming, L.; Herbst-Irmer, R. *Organometallics* **1996**, *15*, 5252. (h) Dohmeier, C.; Schnöckel, H.; Robl, C.; Schneider, U.; Ahlrichs, R. *Angew. Chem.* **1993**, *105*, 1714. (i) Schonberg, P. R.; Paine, R. T.; Campana, C. F. *J. Am. Chem. Soc.* **1976**, *101*, 7726. (j) Schonberg, P. R.; Paine, R. T.; Campana, C. F.; Duesler, E. N. *Organometallics* **1982**, *1*, 799. (k) Koch, H.-J.; Schulz, S.; Roesky, H. W.; Noltemeyer, M.; Schmidt, H.-G.; Heine, A.; Herbst-Irmer, R.; Stalke, D.; Sheldrick, G. M. *Chem. Ber.* **1992**, *125*, 1107. (l) Schulz, S.; Roesky, H. W.; Koch, H.-J.; Sheldrick, G. M.; Stalke, D.; Kuhn, A. *Angew. Chem.* **1993**, *105*, 1828. (m) See also: Jutzi, P.; Dahlhaus, J.

with larger and/or more electronegative substituents have the Cp ring η^5 -bound.^{42c,d} $\text{Me}_5\text{C}_5\text{AlX}_2$ -type complexes with formally three-coordinate Al can have the Cp group η^5 (Al2 and Al3 in $(\text{Me}_5\text{C}_5\text{Al})_6\text{P}_4$ ^{42e}) or σ -bound $([\text{Me}_5\text{C}_5\text{Al}][(\text{Me}_3\text{Si})_2\text{NAl}][\text{NAl}(\text{Me}_5\text{C}_5)_2][\text{NAl}(\text{Me}_5\text{C}_5)(\text{SiMe}_3)]_2$)^{42f}, $(\text{Me}_5\text{C}_5\text{AlNSi}t\text{Bu}_3)_2$ ^{42g}). Similarly, the hapticity can vary significantly in formally four-coordinate $\text{Me}_5\text{C}_5\text{AlX}_3$ -type complexes, depending on the nature of the groups X: σ -bound arrangements are observed for Al1 in $(\text{Me}_5\text{C}_5\text{Al})_6\text{P}_4$ ^{42e} and in $\text{Me}_5\text{C}_5\text{-AlCl}_3^-$,^{42h} an η^3 bonding mode can be observed in $(\text{Me}_5\text{C}_5\text{AlMeCl})_2$ ⁴²ⁱ and $(\text{Me}_5\text{C}_5\text{AlBuCl})_2$,^{42i,j} and more symmetrical η^5 bonding is found in $(\text{RMe}_4\text{C}_5\text{AlCl}_2)_2$ (R = Me, Et)^{42k} and $(\text{Me}_5\text{C}_5\text{AlE})_4$ (E = Se, Te).^{42l} There seems to be a trend here toward increased hapticity for more electronegative, poorly π -donating X groups.^{42m} CpGaMe_2 forms a coordination polymer^{43a} similar to CpAlMe_2 ; the gas-phase structure has not been determined. CpGaEt_2 and Cp_2GaEt form similar chain structures in the solid state.^{43b} $(\text{Me}_5\text{C}_5\text{GaCl}_2)_2$, unlike the analogous Al complex, has σ -bound Cp rings;^{43c} the Cp rings in $(\text{Me}_5\text{C}_5\text{GaNC}_6\text{Me}_2\text{H}_3)_2$ and $(\text{Me}_3\text{Si})_2\text{N}(\text{Me}_5\text{C}_5)\text{GaN}_3$ are also σ -bound.^{43d} In general, Ga complexes tend to have lower hapticities than the corresponding Al complexes. CpInMe_2 ⁴⁴ and Cp_3In form polymeric chain structures in the solid state; the structure of monomeric CpInMe_2 has not been determined. There are no X-ray structures at all of CpTl^{III} derivatives.

Cp_2AlMe has a $\eta^2:\eta^2$ structure^{42p} very similar to the one we calculate for Cp_2AlH , as does $(\text{Me}_5\text{C}_5)_2\text{AlMe}$,^{42o} but the Cp groups in $(\text{Cp}_2\text{AlO}i\text{Pr})_2$ ^{42r} and in the $(\text{Me}_5\text{C}_5)_2\text{-Al}$ fragment of $([\text{Me}_5\text{C}_5\text{Al}][(\text{Me}_3\text{Si})_2\text{NAl}][\text{NAl}(\text{Me}_5\text{C}_5)_2][\text{NAl}(\text{Me}_5\text{C}_5)(\text{SiMe}_3)]_2$)^{42f} are σ -bound. Three tricyclopentadienylaluminum compounds have been reported to date.^{42q} The structure of Cp_3Al contains one molecule with a $\eta^2:\eta^{1.5}:\eta^{1.5}$ arrangement and one that more closely resembles $\eta^2:\eta^{1.5}:\eta^1$, $(\text{Me}_3\text{C}_5\text{H}_2)_3\text{Al}$ is $\eta^5:\sigma:\sigma$, and $(\text{Me}_4\text{-C}_5\text{H})_3\text{Al}$ is $\sigma:\sigma:\sigma$. The variability of the bonding arrangements has been ascribed to a very flat potential for ring slippage, combined with the steric effects of increasing methyl substitution. Cp_3Ga ,^{43e} $(\text{Cp}_2\text{GaOEt})_2$,^{43f} $(\text{Me}_5\text{C}_5)_2\text{-GaCl}_2$,^{43g} and $(\text{Me}_5\text{C}_5)_3\text{Ga}$ ^{43h} all have σ -bound Cp rings.

Group 14. The monocyclopentadienyl cations CpM^+ (M = Si–Pb), isoelectronic with the neutral group 13 derivatives, have similar η^5 structures with large metal–

ring distances. Not surprisingly, the preference for a central η^5 structure is even more pronounced here than for the group 13 elements (CpSi^+ , $A_5 = 0.40 \text{ \AA}^2$; CpAl , $A_5 = 0.92 \text{ \AA}^2$). The dicyclopentadienyls Cp_2M have bent-sandwich structures in which ring slippage decreases but bending stays nearly constant on going from Cp_2Si ($\eta^2:\eta^2$: $\angle\text{Cg-M-Cg} = 155^\circ$, slip 0.72 \AA) to Cp_2Pb (η^4 : η^4 : $\angle\text{Cg-M-Cg} = 155^\circ$, slip 0.24 \AA). The difference in energy between the bent-sandwich structure and the idealized D_{5d} structure is uniformly small (for Si–Pb: 4.1, 0.6, 1.9, 0.6 kcal/mol, respectively). Bending of these species has been the subject of several papers^{1c,45,47c,50f} and will not be discussed in detail here. The divalent complexes CpMH all prefer η^2 -bound structures, with the hydride pointing away from the Cp group. The difference between η^2 and η^3 structures is small (1–2 kcal/mol). The tetravalent species CpMH_3 all prefer purely σ -bound structures with a considerable barrier for ring whizzing via the η^2 structure; this barrier decreases somewhat on going from Si (14 kcal/mol) to Pb (8 kcal/mol). Figure 10 shows the calculated η^2 and η^3/σ structures of CpGeH and CpGeH_3 .

No structures of isolated unsubstituted cations CpM^+ (M = Si–Pb) have been determined, but the structure of $\text{Cp}_3\text{Sn}_2\text{BF}_4(\text{THF})$ contains an η^5 - CpSn unit only weakly bound to a THF molecule and the Cp rings of neighboring Cp_2Sn units.⁴⁶ More substituted Cp^+M^+ derivatives of Ge–Pb invariably show η^5 structures;⁴⁷ no derivatives of CpSi^+ have been reported yet. The X-ray structures of $\text{Me}_5\text{C}_5\text{GeCH}(\text{SiMe}_3)_2$,^{48a} $\text{Me}_5\text{C}_5\text{GeC}(\text{SiMe}_3)_3$,^{48b} $\text{Me}_5\text{C}_5\text{GeC}_6\text{H}_2t\text{Bu}_3$,^{47b} $\text{Me}_5\text{C}_5\text{GeCl}$,^{47b,48c} and $\text{Me}_5\text{C}_5\text{SnCl}$ ^{48d} as well as the transition-metal complexes $\text{Me}_5\text{C}_5\text{Ge}(\text{CH}(\text{SiMe}_3)_2)\text{W}(\text{CO})_5$ ^{48e} and $\text{Me}_5\text{C}_5\text{Ge}(\text{Cl})\text{W}(\text{CO})_5$ ^{48f} have the metal atom η^2 -bound to the Cp ring. The structure of CpSnCl has also been reported,^{48g} but the Cp ring bond lengths and angles clearly indicate the presence of severe disorder in the crystal, making it difficult to establish the mode of bonding of the ring to

(45) (a) Bruno, G.; Ciliberto, E.; Fragalà, I. L. *J. Organomet. Chem.* **1985**, *289*, 263. (b) Schoeller, W. W.; Friedrich, O.; Sundermann, A.; Rozhenko, A. *Organometallics* **1999**, *18*, 2099.

(46) Dory, T. S.; Zuckerman, J. J.; Barnes, C. L. *J. Organomet. Chem.* **1985**, *281*, C1.

(47) (a) Hani, R.; Geanangel, R. A. *J. Organomet. Chem.* **1985**, *293*, 197 ($t\text{BuC}_6\text{H}_4\text{Sn}^+$). (b) Winter, J. G.; Portius, P.; Kociok-Köhn, G.; Steck, R.; Filippou, A. C. *Organometallics* **1998**, *17*, 4176 ($\text{Me}_5\text{C}_5\text{Ge}^+$). (c) Jutzi, P.; Kohl, F.; Hofmann, P.; Krüger, C.; Tsay, Y.-H. *Chem. Ber.* **1980**, *113*, 757 ($\text{Me}_5\text{C}_5\text{Sn}^+$). (d) Jutzi, P.; Dickbreder, R.; Nöth, H. *Chem. Ber.* **1989**, *122*, 865 ($\text{Me}_5\text{C}_5\text{Pb}^+$).

(48) (a) Jutzi, P.; Hampel, B.; Hursthouse, M. B.; Howes, A. J. *Organometallics* **1986**, *5*, 1944. (b) Jutzi, P.; Becker, A.; Leue, C.; Stammler, H. G.; Neumann, B.; Hursthouse, M. B.; Karaulov, A. *Organometallics* **1991**, *10*, 3838. (c) Fernholt, L.; Haaland, A.; Jutzi, P.; Kohl, F. X.; Seip, R. *Acta Chem. Scand.* **1984**, *A38*, 211. (d) Constantine, S. P.; De Lima, G. M.; Hitchcock, P. B.; Keates, J. M.; Lawless, G. A.; Marziano, I. *Organometallics* **1997**, *16*, 793. (e) Jutzi, P.; Hampel, B.; Hursthouse, M. B.; Howes, A. J. *J. Organomet. Chem.* **1986**, *299*, 19. (f) Jutzi, P.; Hampel, B.; Stroppel, K.; Krüger, C.; Angermund, K.; Hofmann, P. *Chem. Ber.* **1985**, *118*, 2789. (g) Bos, C. D.; Bulten, E. J.; Noltes, J. G.; Spek, A. L. *J. Organomet. Chem.* **1975**, *99*, 71.

(49) (a) Jutzi, P.; Kanne, D.; Krüger, C. *Angew. Chem.* **1986**, *98*, 163. (b) Jutzi, P.; Holtmann, U.; Kanne, D.; Krüger, C.; Blom, R.; Gleiter, R.; Hyla-Krispin, I. *Chem. Ber.* **1989**, *122*, 1629.

(50) (a) Grenz, M.; Hahn, E.; Du Mont, W.-W.; Pickardt, J. *Angew. Chem.* **1984**, *96*, 69. (b) Almlöf, J.; Fernholt, L.; Fægri, K., Jr.; Haaland, A.; Schilling, B. E. R.; Seip, R.; Taubøl, K. *Acta Chem. Scand.* **1983**, *A37*, 131. (c) Schumann, H.; Janiak, C.; Hahn, E.; Loebel, J.; Zuckerman, J. J. *Angew. Chem.* **1985**, *97*, 765. (d) Jutzi, P.; Schlüter, E.; Hursthouse, M. B.; Arif, A. M.; Short, R. L. *J. Organomet. Chem.* **1986**, *299*, 285. (e) Schumann, H.; Janiak, C.; Hahn, E.; Kolax, C.; Loebel, J.; Rausch, M. D.; Zuckerman, J. J.; Heeg, M. J. *Chem. Ber.* **1986**, *119*, 2656. (f) Constantine, S. P.; Cox, H.; Hitchcock, P. B.; Lawless, G. A. *Organometallics* **2000**, *19*, 317.

Neumann, B.; Stammler, H.-G. *Organometallics* **1996**, *15*, 747. (n) Burns, C. T.; Stelck, D. S.; Shapiro, P. J.; Vij, A.; Kunz, K.; Kehr, G.; Concolino, T.; Rheingold, A. L. *Organometallics* **1999**, *18*, 5432. (o) Burns, C. T.; Shapiro, P. J.; Budzelaar, P. H. M.; Willett, R.; Vij, A. *Organometallics* **2000**, *19*, 3361. (p) Fisher, J. D.; Wei, M.-Y.; Willett, R.; Shapiro, P. J. *Organometallics* **1994**, *13*, 3324. (q) Fisher, J. D.; Budzelaar, P. H. M.; Shapiro, P. J.; Staples, R. J.; Yap, G. A.; Rheingold, A. L. *Organometallics* **1997**, *16*, 871. (r) Kunicki, A.; Sadowski, R.; Zachara, J. *J. Organomet. Chem.* **1996**, *508*, 249.

(43) (a) Mertz, K.; Zettler, F.; Hausen, H. D.; Weidlein, J. J. *Organomet. Chem.* **1976**, *122*, 159. (b) Beachley, O. T., Jr.; Rosenblum, D. B.; Churchill, M. R.; Lake, C. H.; Krajkowski, L. M. *Organometallics* **1995**, *14*, 4402. (c) Beachley, O. T., Jr.; Hallock, R. B.; Zhang, H. M.; Atwood, J. L. *Organometallics* **1985**, *4*, 1675. (d) Jutzi, P.; Neumann, B.; Reumann, G.; Stammler, H.-G. *Organometallics* **1999**, *18*, 2037. (e) Beachley, O. T., Jr.; Getman, T. D.; Kirss, R. U.; Hallock, R. B.; Hunter, W. E.; Atwood, J. L. *Organometallics* **1985**, *4*, 751. (f) Cowley, A. H.; Mehrotra, S. K.; Atwood, J. L.; Hunter, W. E. *Organometallics* **1985**, *4*, 1115. (g) Beachley, O. T., Jr.; Hallock, R. B.; Zhang, H. M.; Atwood, J. L. *Organometallics* **1985**, *4*, 1675. (h) Schumann, H.; Nickel, S.; Weimann, R. *J. Organomet. Chem.* **1994**, *468*, 43.

(44) (a) Beachley, O. T., Jr.; Robirds, E. S.; Atwood, D. A.; Wei, P. *Organometallics* **1999**, *18*, 2561. (b) Einstein, F. W. B.; Gilbert, M. M.; Tuck, D. G. *Inorg. Chem.* **1972**, *11*, 2833.

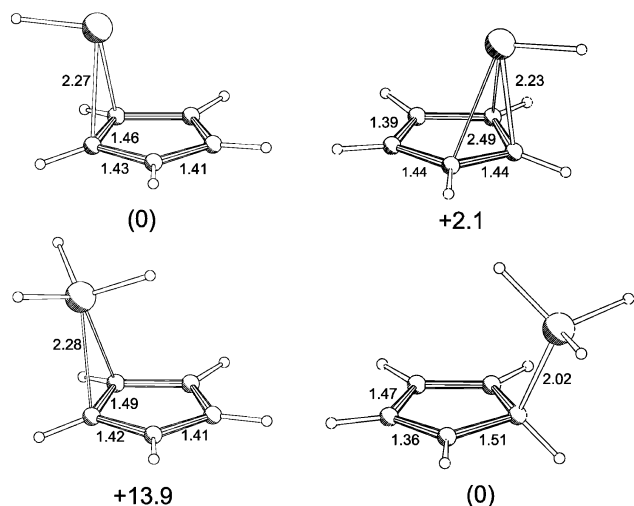


Figure 10. Calculated η^2 and η^3/σ structures for CpGeH and CpGeH₃.

the metal. Cp₂Si is unknown; the unit cell of (Me₅C₅)₂-Si contains two independent molecules, one of which is bent but the other has strictly parallel rings.⁴⁹ Monomeric Cp₂Ge^{50a} and Cp₂Sn^{51a,52a} have the expected bent-sandwich structure; substituents on the Cp ring tend to reduce the degree of bending.^{50b–f,51b–d} Cp₂Pb is polymeric^{52b–d} or oligomeric^{52c} in the solid state, but in the gas phase it adopts a bent-sandwich structure;^{52a} substituted derivatives have sandwich structures with variable degrees of bending.^{50e,f,51a,52e–g} Metal(IV) cyclopentadienyls of Si–Pb invariably have η^1 or σ -bound Cp rings,^{53a–i} although fluxionality of the ring is frequently observed in solution.^{53j}

Group 15. Cationic metallocenes Cp₂M⁺ of As and Sb prefer slipped bent-sandwich structures which are best described as $\eta^2:\eta^2$, similar to Cp₂Si. Cp₂Bi⁺ prefers a symmetrical *D*_{5d} structure, i.e., with a stereochemically inactive lone pair. The cations CpMH⁺ (M = As–Bi) all prefer an η^2 structure (H away from Cp) to the η^3 alternative; the preference decreases on going down

the periodic table from As (6 kcal/mol) to Bi (3 kcal/mol). Neutral species Cp₂MH all have a $\sigma:\sigma$ structure. Dihydrides CpMH₂ are likewise σ -bound, with the hydrides pointing away from the Cp group; the barrier for ring whizzing decreases from As (17 kcal/mol) to Bi (8 kcal/mol).

Metallocenium type bent-sandwich structures have been observed for (Me₅C₅)₂As⁺,⁵⁴ (Me₅C₅)₂Sb⁺, and (tBu₃C₅H₂)₂Sb⁺,⁵⁵ the bismuth analogue (tBu₃C₅H₂)₂Bi⁺ has nearly parallel $\eta^5:\eta^5$ -bound Cp rings.⁵⁶ (Me₅C₅)-PNH/tBu⁺ has an η^2 -bound Cp ring. The structures of Cp₃Sb⁵⁷ and Cp₃Bi⁵⁸ each contain three σ -bound Cp rings. The monocyclopentadienyl derivatives (tPr₄C₅H)-MCl₂ show a gradual change from σ to η^1/η^3 type metal–Cp interactions on going from P to Bi and a decreasing barrier for ring whizzing.⁵⁹

Comparison with Transition Metals. To put our results in perspective, we have also included a few transition-metal complexes. The slippage curves for typical saturated 18e complexes Cp₂Fe and CpMn(CO)₃ (see Figure 4) are *much* steeper than those for any main-group metal, as is also demonstrated by their small *A*₅ values of 0.20 and 0.26 Å², respectively (cf. Cp₂Mg, 1.3 Å²; CpMgH, 0.92 Å²). This illustrates the strength of the π -component of the bonding in these complexes: σ -type interactions can be maintained up to relatively large slippage distances, but even a modest slippage already results in loss of at least one π -interaction. On the other hand, the high-spin Mn^{II} derivatives CpMnH (*A*₅ = 0.99 Å²) and Cp₂Mn (*A*₅ = 1.8 Å²) have much softer curves (also included in Figure 4) rather similar to those of their magnesium counterparts, as expected for a largely ionic metal–ring interaction.

Discussion

Ionic vs Covalent Bonding. Cyclopentadienyls of Li, Na, and Mg are probably best described as mainly ionic.^{1c} As a consequence, the structures exhibit the highest hapticity compatible with steric constraints. Complexes of Be and Al are borderline. The $\eta^5:\eta^5$ structure of Cp₂Al⁺ and the nearly free movement in CpAlH₂ of the AlH₂ fragment over the ring surface indicate that excess-electron structures are easily accessible, which is easily explained by a high degree of ionicity in the metal–Cp bond. For Cp₂Be, it is probable that both partial covalency and steric effects destabilize the $\eta^5:\eta^5$ arrangement and so combine to give an

(51) (a) Atwood, J. L.; Hunter, W. E.; Cowley, A. H.; Jones, R. A.; Stewart, C. A. *J. Chem. Soc., Chem. Commun.* **1981**, 925. (b) Heeg, M. J.; Herber, R. H.; Janiak, C.; Zuckerman, J. J.; Schumann, H.; Manders, W. F. *J. Organomet. Chem.* **1988**, 346, 321. (c) Heeg, M. J.; Zuckerman, J. J. *J. Am. Chem. Soc.* **1984**, 106, 4259. (d) Burkey, D. J.; Hanusa, T. P. *Organometallics* **1995**, 14, 11.

(52) (a) Almenningen, A.; Haaland, A.; Motzfeldt, T. *J. Organomet. Chem.* **1967**, 7, 97. (b) Panattoni, C.; Bombieri, G.; Croatto, U. *Acta Crystallogr.* **1966**, 21, 823. (c) Beswick, M. A.; Lopez-Casideo, C.; Paver, M. A.; Raithby, P. R.; Russell, C. A.; Steiner, A.; Wright, D. S. *Chem. Commun.* **1997**, 109. (d) Overby, J. S.; Hanusa, T. P.; Young, V. G., Jr. *Inorg. Chem.* **1998**, 37, 163. (e) Constantine, S. P.; Hitchcock, P. B.; Lawless, G. A. *Organometallics* **1996**, 15, 3905. (f) Sitzmann, H. *Z. Anorg. Allg. Chem.* **1995**, 621, 553. (g) Evans, W. J.; Clark, R. D.; Forrestal, K. J.; Ziller, J. W. *Organometallics* **1999**, 18, 2401.

(53) (a) Jutzi, P.; Kanne, D.; Hursthouse, M.; Howes, A. J. *Chem. Ber.* **1988**, 121, 1299 (Me₅C₅)₂SiF₂, (Me₅C₅)₂SiCl₂. (b) Jutzi, P.; Strassburger, G.; Schneider, M.; Stammli, H.-G.; Neumann, B. *Organometallics* **1996**, 15, 2842 (Me₅C₅Si(OH)₃). (c) Kulishov, V. I.; Bokii, N. G.; Prikhot'ko, A. F.; Struchkov, Y. T. *Z. Strukt. Khim.* **1975**, 16, 252 (Cp₄Sn). (d) Kulishov, V. I.; Rodé, G. G.; Bokii, N. G.; Prikhot'ko, A. F.; Struchkov, Y. T. *Z. Strukt. Khim.* **1975**, 16, 247 (1,1-C₅H₄(SnMe₃)₂). (e) Janiak, C.; Weimann, R.; Görlitz, F. *Organometallics* **1997**, 16, 4933 (Ph₃C₅SnCl₃). (f) Gaffney, C.; Harrison, P. G. *J. Chem. Soc., Dalton Trans.* **1982**, 1055 (CpPbPh₃). (g) Winter, J. G.; Portius, P.; Kociok-Kohn, G.; Steck, R.; Filippou, A. C. *Organometallics* **1998**, 17, 4176 (CpGeH₃). (h) Enders, M.; Rudolph, R.; Pritzkow, H. *J. Organomet. Chem.* **1997**, 549, 251 (ArMe₂C₅H₂SiMe₃). (i) Rufanov, K. A.; Churakov, A. V.; Kazennova, N. B.; Brusova, G. P.; Lemenovskii, D. A.; Kuz'mina, L. G. *J. Organomet. Chem.* **1995**, 498, 37 (Ph₃CC₅H₄-SnMe₃). (j) See e.g.: Grimmond, B. J.; Corey, J. Y. *Organometallics* **1999**, 18, 4646.

(54) Jutzi, P.; Wippermann, T.; Krüger, C.; Kraus, H. *J. Angew. Chem.* **1983**, 95, 244.

(55) Sitzmann, H.; Ehleiter, Y.; Wolmershäuser, G.; Ecker, A.; Üffing, C.; Schnöckel, H. *J. Organomet. Chem.* **1997**, 527, 209.

(56) Sitzmann, H.; Wolmershäuser, G. *Z. Naturforsch.* **1997**, B52, 398.

(57) Birkhahn, M.; Krommes, P.; Massa, W.; Lorberth, J. *J. Organomet. Chem.* **1981**, 208, 161.

(58) Lorberth, J.; Massa, W.; Wocadlo, S.; Sarraje, I.; Shin, S.-H. *J. Organomet. Chem.* **1995**, 485, 149.

(59) Ehleiter, Y.; Sitzmann, H.; Boese, R. *Z. Anorg. Allg. Chem.* **1996**, 622, 923.

(60) Jutzi, P.; Pilotek, S.; Neumann, B.; Stammli, H.-G. *J. Organomet. Chem.* **1998**, 552, 221.

(61) Kekia, O. M.; Jones, R. L., Jr.; Rheingold, A. L. *Organometallics* **1996**, 15, 4104.

(62) Sitzmann, H.; Wolmershäuser, G. *Chem. Ber.* **1994**, 127, 1335.

(63) Hebandanz, N.; Kohler, F. H.; Müller, G.; Riede, J. *J. Am. Chem. Soc.* **1986**, 108, 3281.

(64) Cowie, J.; Hamilton, E. J. M.; Laurie, J. C. V.; Welch, A. J. *J. Organomet. Chem.* **1990**, 394, 1.

(65) Brock, C. P.; Fu, Y. *Acta Crystallogr.* **1997**, C53, 928.

Table 3. VB Results for CpAlH₂, CpSiH, and CpSiH₃

	structure			resonance energy			total energy
	ionic	σ	π	ionic- σ	ionic- π	σ - π	
CpAlH ₂ η^3	-435.01299	-435.05297	-434.99240	-0.19576	-0.07496	-0.08808	-435.18550
weights	0.311	0.439	0.250				
orbital overlap		0.546	0.369				
CpAlH ₂ η^2	-435.01599	-435.08241	-434.99620	-0.207473	-0.06013	-0.07176	-435.19443
weights	0.303	0.482	0.215				
orbital overlap		0.569	0.331				
CpSiH η^3	-481.38890	-481.42433	-481.43019	-0.156548	-0.07218	-0.07189	-481.57726
weights	0.286	0.383	0.331				
orbital overlap		0.454	0.334				
CpSiH η^2	-481.40248	-481.45133	-481.43839	-0.169704	-0.06264	-0.06709	-481.59089
weights	0.287	0.413	0.300				
orbital overlap		0.490	0.314				
CpSiH ₃ η^1	-482.53598	-482.74058		-0.309491			-482.78394
weights	0.260	0.740					
orbital overlap		0.595					
CpSiH ₃ η^2	-482.54359	-482.66160		-0.257657			-482.72676
weights	0.343	0.657					
orbital overlap		0.521					

electron-precise structure as the global minimum. For all other metals studied, the observed structures are probably best interpreted in covalent terms. This does not mean that the contribution of ionicity will be unimportant. *All* elements included in this study are more electropositive than carbon. Indeed, extensive studies by Rayón and Frenking show that, except for boron, most of the Cp-metal bonding energy is due to the electrostatic component of the bonding.^{1c} Since, however, covalent interactions are much more directional, they can easily dominate in determining structure and hapticity even if their energy contribution is relatively modest.

η^5 or a Lower Hapticity? Even though we are going to describe metal-Cp bonding in covalent terms, it is most convenient to start with a Cp *anion* and a positively charged metal fragment. Bonds are then formed by donation of electrons from the Cp group to the metal. The orbitals involved in the metal-ring bonding are the three Cp π orbitals (π_1 , π_{2a} , π_{2b}) and the metal *ns* and *np* orbitals. To interpret the results described earlier, we have to distinguish between systems with an initially empty *ns* orbital (Cu⁺, Zn²⁺) and an initially filled *ns* orbital (Al⁺, Si²⁺). Intermediate situations occur if the *ns* orbital is partially occupied because it is involved in bonding within the metal fragment (CuPH₃⁺, ZnH⁺).

If the metal *ns* orbital was originally empty, it will form the strongest bond to the Cp anion. Since the best overlap is obtained in an η^1 - or σ -bound situation, this results in a preference for a localized interaction with a single carbon. Of course, the metal *np* orbitals are empty as well and can form additional π -bonds to the ring in an η^5 situation. However, of the relevant systems (Cu⁺-Au⁺, Zn²⁺-Hg²⁺), only Cu⁺ forms π -bonds that are strong enough to compensate for the partial loss of σ -bonding in the η^5 structure, resulting in nearly free movement of Cu over the ring plane. Moving both down (to Au⁺) and to the right (to Zn²⁺) in the periodic table makes the competition of the p_π orbitals less effective, resulting in a preference for localized bonding.

The situation changes if a σ -donor is added to the metal (e.g. PH₃ to Cu⁺ or H⁻ to Zn²⁺). This makes the metal *ns* orbital a weaker acceptor for Cp electron density and hence *decreases* the preference for σ -bond-

ing. As a result, CpAg·PH₃, CpZnH, and CpCdH are η^5 -bound, whereas CpAg, CpZn⁺, and CpCd⁺ were not. The somewhat counterintuitive result that adding a donor can increase the hapticity of the complex is best explained by noting that the effect of the σ -donor on the σ -system, which opposes η^5 -bonding, is *direct*, whereas the effect on the metal p_π -acceptor orbitals, which favor η^5 -bonding, is only *indirect*.

If the metal *ns* orbital was originally full (i.e. it was a metal-centered lone pair), it will have a repulsive interaction with the ring π orbitals, resulting in a large metal-Cp distance. The metal-Cp bond is now mainly formed by metal *np* orbitals. Since the p_π interaction is not much weaker than the p_σ interaction, a strong preference for high hapticity is observed in the mono-Cp derivatives of Al⁺-Ti⁺ and Si²⁺-Pb²⁺. Formal protonation of the metal *ns* lone pair to form an M-H bond reduces its repulsion with the Cp ring. This results not only in shorter Cp-M distances but also in an increased preference for a localized interaction, because the *ns* orbital can now participate in the metal-Cp bond. Thus, CpTiH⁺ prefers an η^1 -bound structure, while CpTi is η^5 .

In the bis-Cp derivatives of Si²⁺-Pb²⁺, having two η^5 -bound Cp rings would result in electron-excess structures. This is avoided in Cp₂Si by ring slippage to a η^2 : η^2 structure. In Cp₂Pb, where the interaction is somewhat more ionic, having an excess-electron structure is less of a problem, and a structure closer to η^5 : η^5 results. Similar trends are seen in Cp₂M⁺ (M = As-Bi). In all of these structures, M-Cp distances are relatively large because of M *ns*-Cp π repulsion.

Regardless of the initial state of the of the metal *ns* orbital, if metal *np* π -acceptor orbitals are blocked by additional electron-pair donors a lower hapticity always results. Clear examples of this effect are CpZnH (η^5) → CpZnH₂⁻/CpAlH₂ (η^2), CpSn⁺ (η^5) → CpSnH/CpSbH⁺ (η^2), and CpAlH₂ (η^2) → CpAlH₃⁻/CpSiH₃ (σ). Thus, as long as the Cp-M bond is not too ionic, electron-counting rules can at least be used to predict an *upper limit* to the hapticity.

Throughout the periodic table we consistently see a "softer" Cp-metal bond on going down a group. In most cases the heavier elements show a tendency toward lower hapticity, but in a few cases (in particular for

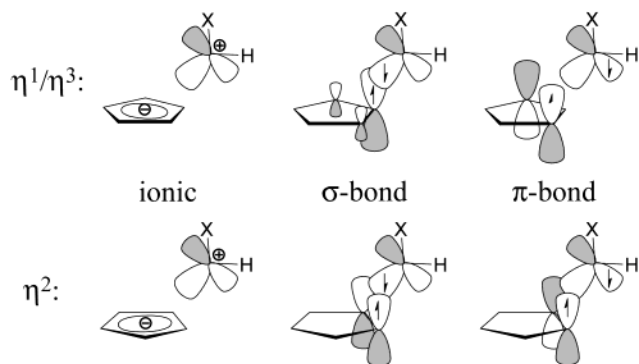


Figure 11. Schematic representations of electronic structures used in VB calculations. X = H for CpAlH₂ or the Si lone pair for CpSiH.

electropositive elements such as Pb and Bi) the opposite trend is sometimes observed.

η^2 vs η^3 Bonding. In most cases where a metal fragment bound to a Cp ring still has one empty p_π orbital, a structure intermediate between η^5 and σ is observed. Examples include CpMH₂ (M = Al–Tl), CpMH (M = Si–Pb), and CpMH⁺ (M = As–Bi). In principle, one could expect either an η^3 or an η^2 structure. However, examples of η^3 structures are rather rare, and our calculations indicate that η^2 structures are uniformly preferred on electronic grounds. How can this be explained?

In MO terms, the two types of structures are nearly equivalent: they just correspond to a choice between the two initially degenerate π orbitals π_{2a} and π_{2b} of the Cp fragment. Of course, the fact that the two orbitals are degenerate does not mean they have the same overlap with a peripherally bound metal fragment in the two situations. Also, the system will deform after bonding to localize ring π bonds and overlaps, and this may be different for the two choices. Nevertheless, it is not easy to rationalize the observed η^2 preference in MO terms. We turned to a VB description of the metal–ring interaction, in the hope that this can provide a clearer picture.

The species CpAlH₂, CpSiH, and CpSiH₃ were used as model compounds. The fragment–ring interaction can be described by the three VB electronic structures shown in Figure 11, which we shall call ionic, σ bond, and π bond (obviously, there is no π bond structure for CpSiH₃). These structures contribute significantly in the VB calculations. Structures with *simultaneous* σ and π fragment–ring bonds or structures with a positive charge on the Cp ring were found to be unimportant. Thus, the Cp–metal interaction must be described as a *single* bond with partial σ and partial π character.

Relevant data (energies, overlaps) have been collected in Table 3. For both CpAlH₂ and CpSiH, the π bond structures have almost the same energy for the η^2 and η^3 arrangements. Both the ionic and the σ bond structures are, however, significantly lower in energy for the η^2 arrangement. For the ionic structure, this may be due to a closer contact between the fragment and the ring. For the σ bond structure, the larger orbital overlap in the η^2 geometry may contribute; the CpSiH orbital drawings in Figure 12 clearly illustrate the better σ overlap in the η^2 geometry and the better π overlap in the η^3 geometry. For CpAlH₂, the ionic structures are

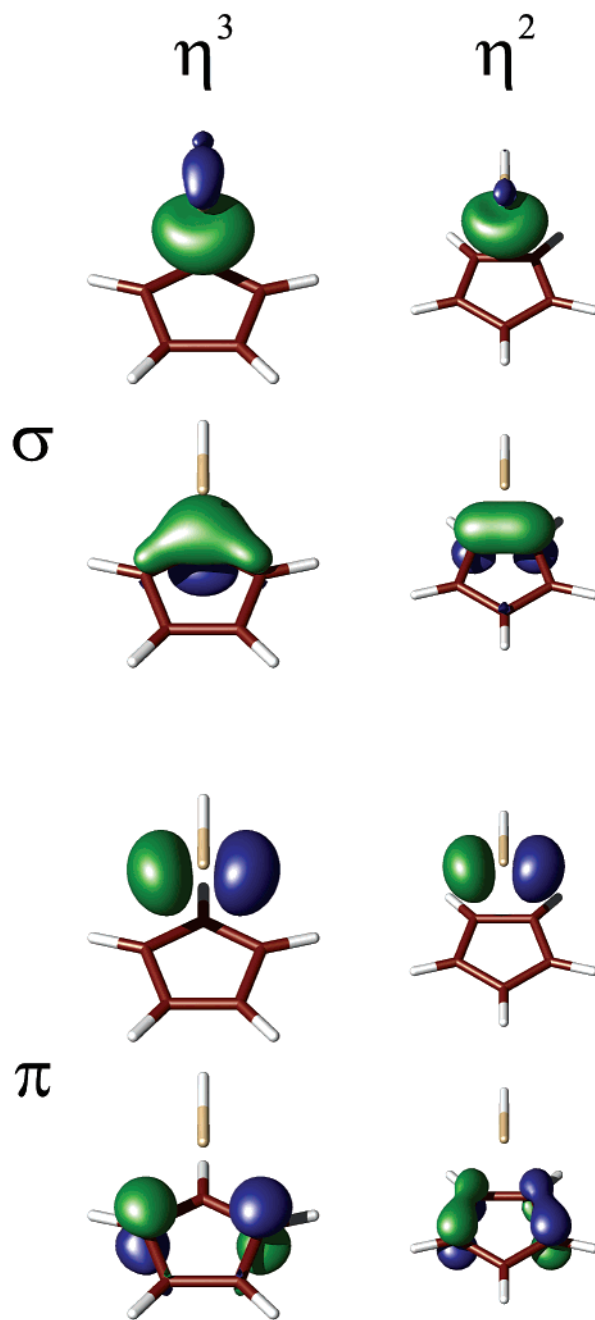


Figure 12. VB orbitals for η^3 - and η^2 -bonded geometries of CpSiH.

intermediate in stability between the σ and π structures; for CpSiH, the ionic structures are the least stable ones. The ionic- σ resonance contribution favors the η^2 geometry, but both resonances involving the π structure favor the η^3 geometry. The net effect of these counteracting contributions is a small preference for the η^2 geometry.

For CpSiH₃, the situation is quite different. There is no π bond structure, and the σ bond structure is always much more stable than the ionic structure. The ionic structure has a slight preference for the η^2 geometry, but the σ bond structure is *much* lower in energy for the η^1 arrangement. This strong preference might be due to the significantly larger orbital overlap (see Table 3) in the η^1 geometry. Possibly, the improved overlap in the η^2 case for CpAlH₂ and CpSiH, but *not* for CpSiH₃, is due to the different composition of the fragment orbital used for metal–ring bonding. In the

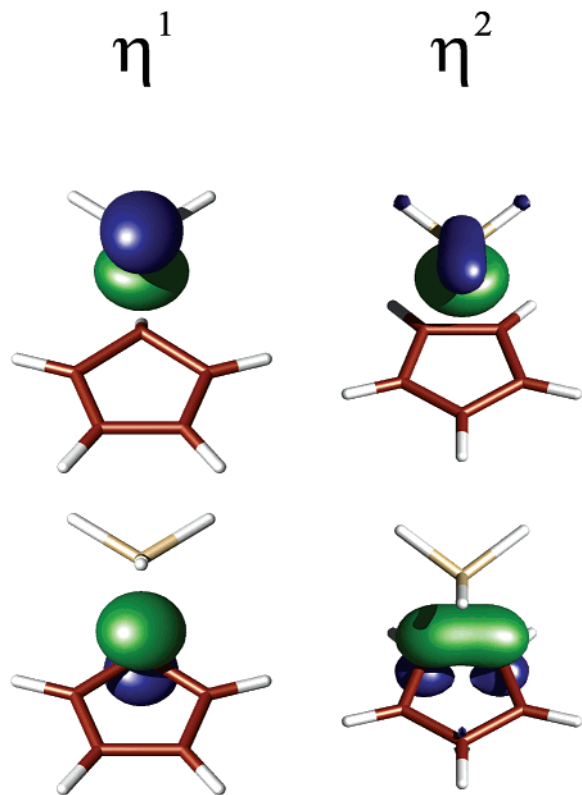


Figure 13. VB orbitals for η^1 - and η^2 -bonded geometries of CpSiH₃.

former two cases, it is an sp^2 hybrid, which is relatively diffuse and hence overlaps well with a partner composed of two ring p_π orbitals. In the case of CpSiH₃, it is an sp^3 hybrid, which is more concentrated and hence overlaps better with a single carbon sp^3 hybrid. The orbital drawings in Figure 13 illustrate the better match in orbital sizes for the η^1 arrangement.

In any case, the VB calculations indicate that, although π bonding is important in unsaturated species such as CpAlH₂ and CpSiH, it is not the main factor in causing the η^2 geometry. Rather, the σ bond and ionic contributions appear to be responsible for the general preference for η^2 structures.

Cp Deformations during Ring Slippage. As the metal fragment moves over the Cp ring, the ring deforms, resulting in unequal C–C bond lengths. The bond length changes seen during ring slippage are readily correlated with electronic interactions: π orbitals that are involved in metal–ring interactions become depopulated (compared to Cp[−]), resulting in elongation of the C–C bonds for which those orbitals are bonding. These changes can be seen in Figures 6 and 8–10. They are rather modest (typically 0.02–0.06 Å, always less than 0.1 Å), close to the error margins of many X-ray structure determinations. In addition, X-ray structures of Cp–main-group-metal compounds often suffer from

disorder problems, which may not always have been recognized. Thus, the practical use of Cp C–C bond lengths as indicators of metal–Cp interactions is probably limited. Certainly, large deformations such as the ca. 0.2 Å reported for CpSnCl^{48g} must be due to crystallographic problems rather than real structural effects.

Conclusions

The theoretical study of a large number of main-group-metal cyclopentadienyls has allowed us to extract some general trends and explain these in terms of ionic contributions and orbital interactions.

Ionic bonding dominates in Li, Na, and Mg derivatives and leads to structures of maximum hapticity. Al is a borderline case, where enough ionic character exists to sometimes form electron-excess structures; this may also be true for some Pb and Bi compounds. In all other cases, electron-precise or electron-deficient structures are formed, where the precise hapticity depends on several factors. If the metal initially has a doubly filled ns orbital, a long Cp–MM bond results, and hapticities are as high as permitted by the electron count (CpGa, CpSn⁺: η^5). If the metal ns orbital is only incompletely filled, it starts to participate in the Cp–MM bonding, causing an increased preference for localized bonding, especially for the heavier elements (CpCu·PH₃, CpZnH, and CpGaH⁺ are all η^5 , but CpAu·PH₃, CpHgH, and CpTIH⁺ are σ or η^1). If the metal ns orbital was originally empty, the preference for a localized bond becomes rather strong (CpCu is still marginally η^5 , CpZn⁺ is η^2 , and CpAg is η^1). On going down a group, we always find a softer Cp–M interaction (shallower slippage curve) and usually also a trend toward more localized bonding.

The wide variety of structures observed in these main-group-metal cyclopentadienyls is caused by the rather different metal–ring bonding preferences of the metal ns and np orbitals. In the transition-metal series, the different types of interactions are much better balanced, causing a nearly uniform η^5 preference. Main-group-metal orbitals are generally more suitable for formation of σ -bonds than of π -bonds. This may also explain the frequent observation of polymeric structures in the solid state.

Acknowledgment. We thank Prof. P. J. Shapiro (University of Idaho) for helpful discussions and the Dutch National Computing Facility (NCF) and the CIMCF (University of Naples) for computer time and technical assistance.

Supporting Information Available: Total energies for optimized species (Table S1) and slippage curves (Table S2). This material is available free of charge via the Internet at <http://pubs.acs.org>.

OM020928V